Seismic imaging from ambient noise, earthquake surface waves and body waves

Huajian Yao
(hjyao@ustc.edu.cn)

University of Science and Technology of China (USTC)

With contributions from:

Hongjian FANG, Cheng LI, Haijiang ZHANG, Yin LIU (USTC)
Rob D. van der Hilst, Pierre Gouedard (MIT), Maarten de Hoop (Purdue Univ)
Yu-Chih HUANG (IES, Academia Sinica, Taiwan)

2015 Cargese workshop

Outline

- Joint ambient noise and earthquake surface wave tomography (isotropic and anisotropic crust and upper mantle structures)

- Direct ambient noise/surface wave travel time tomography with ray tracing and wavelet-based inversion

- Joint ambient noise and body wave travel time tomography

Primary Goal: enhance the resolution and reliability of seismic images, and better understand tectonics and dynamics of Earth's interior

Outline

- **Joint ambient noise and earthquake surface wave tomography (isotropic and anisotropic crust and upper mantle structures)**

- Direct ambient noise/surface wave travel time tomography with ray tracing and wavelet-based inversion

- Joint ambient noise and body wave travel time tomography

Ambient Noise Cross-Correlation

Z-Z → Rayleigh T-T → Love

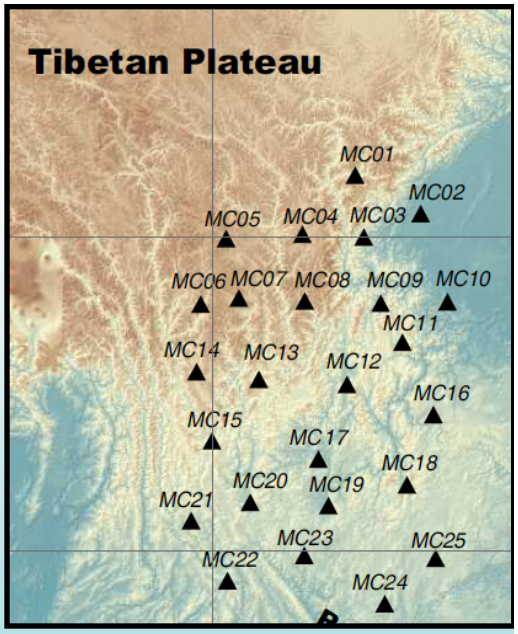

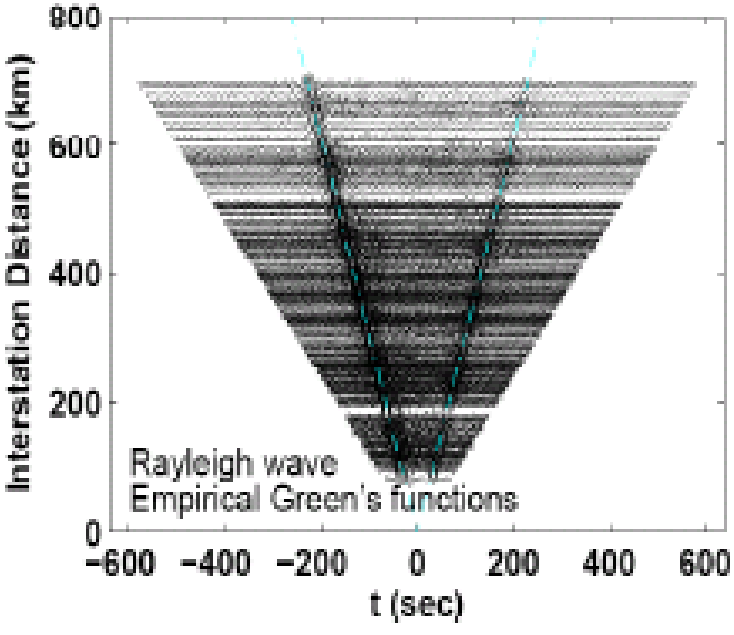

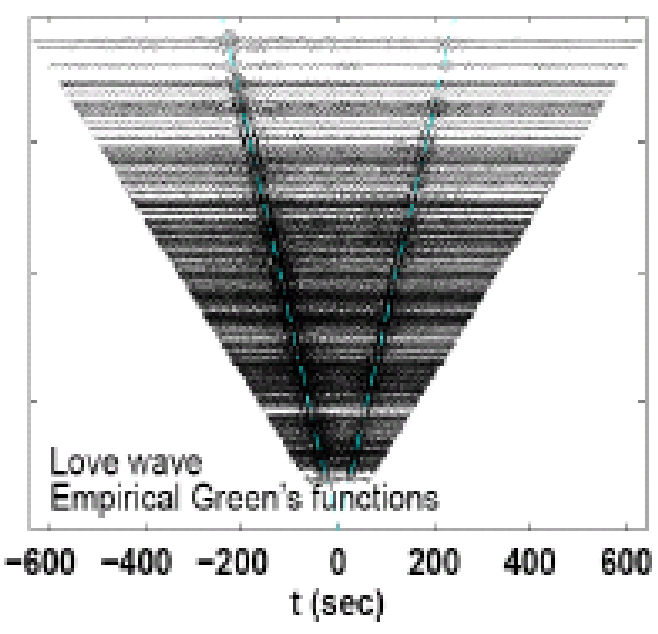

Inter-station ambient noise cross-correlation (5 – 40 s)
→ Surface wave propagation between stations
→ Vsv / Vsh crustal structure beneath the array

Group and Phase Velocity Dispersion Measurements

$$\mathrm{Re}\{G_{AB}(\omega)\exp(-i\omega t)\} \approx (8\pi kS)^{-1/2}\cos\left(k_{AB}\Delta - \omega t + \frac{\pi}{4}\right)$$

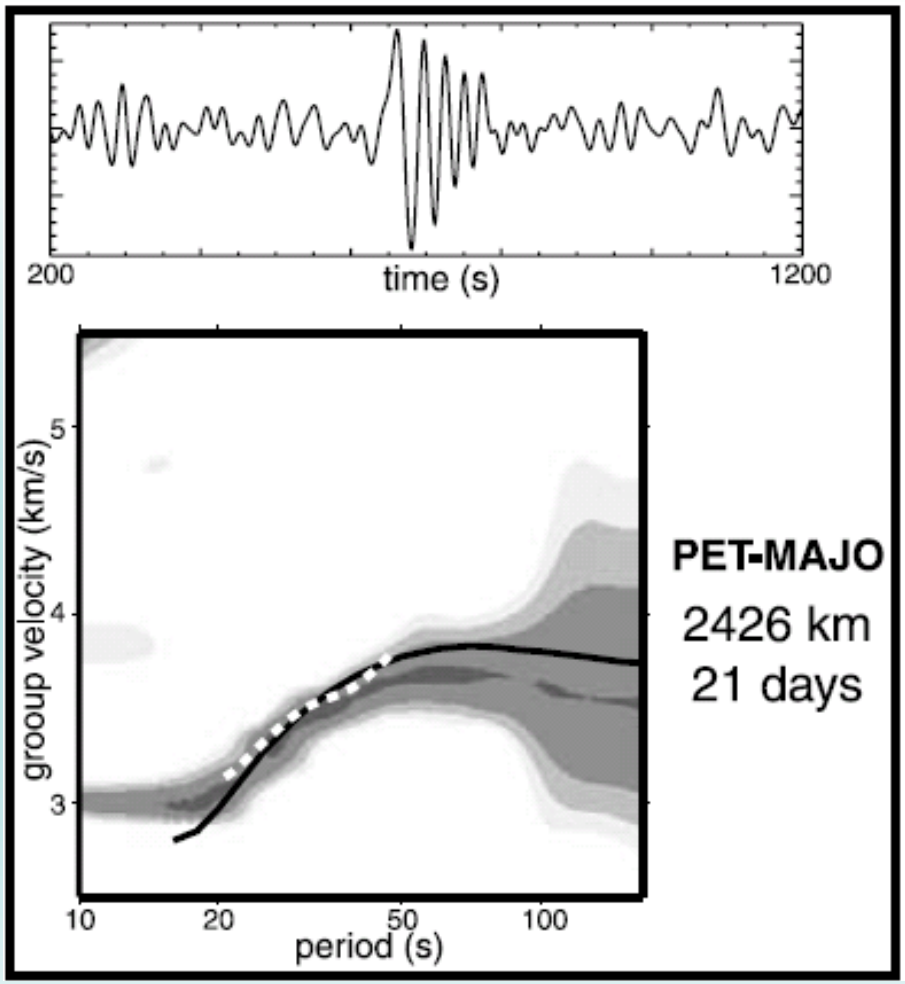

Shapiro & Campillo, GRL, 2004

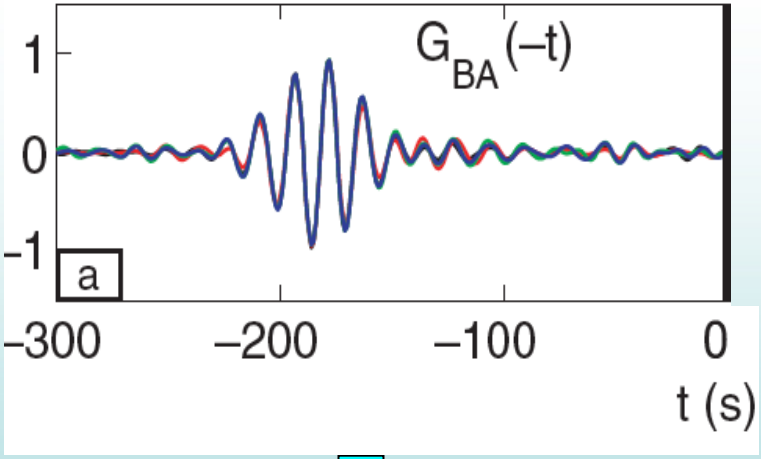

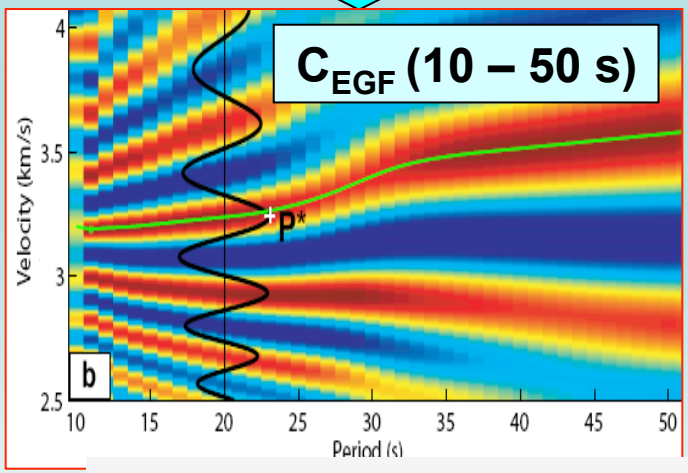

Yao, van der Hilst, de Hoop, 2006, GJI

Monthly Rayleigh wave phase velocity maps from vertical component EGFs

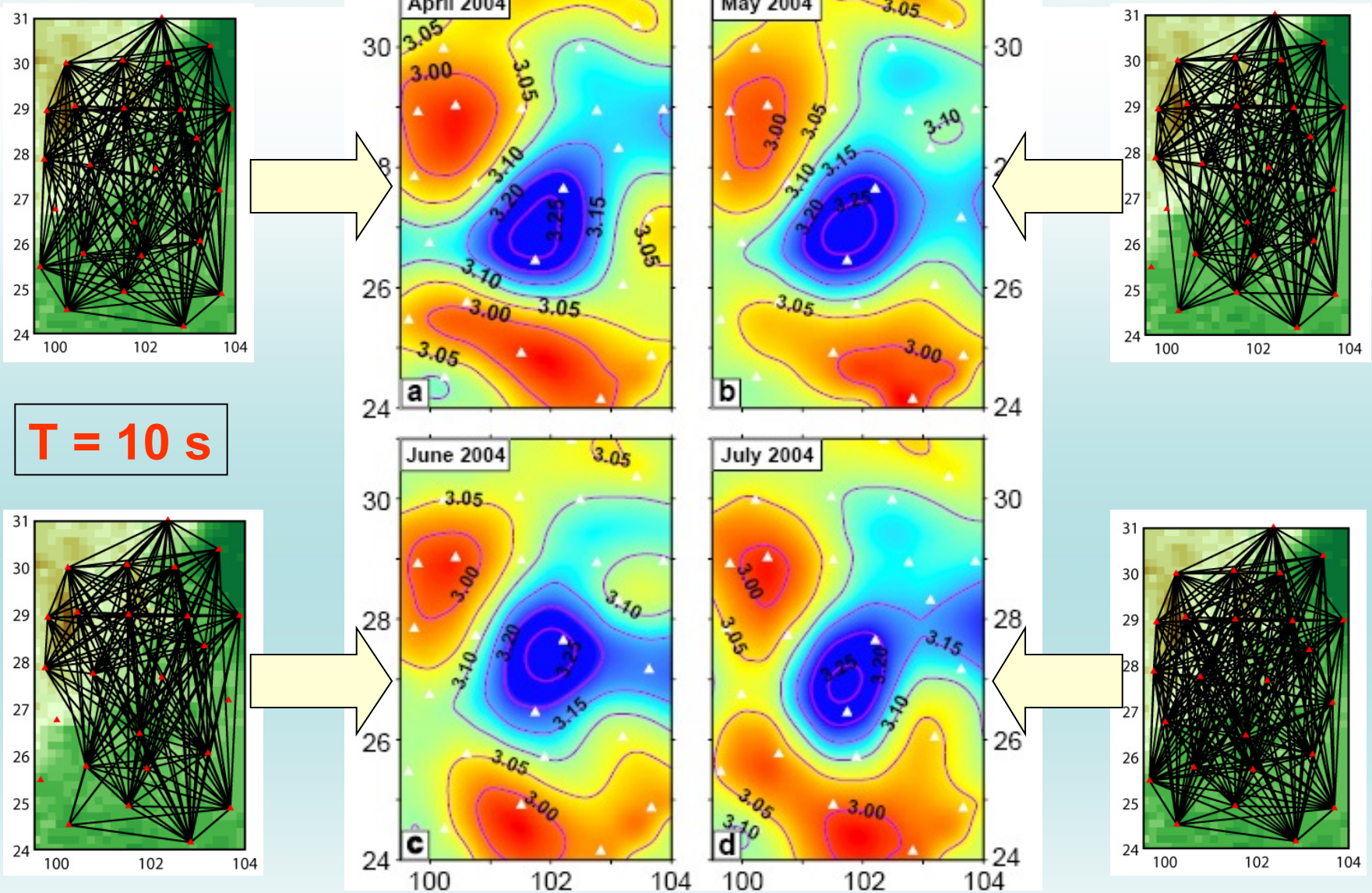

Yao, van der Hilst, de Hoop, 2006

Earthquake Data: Two-station analysis

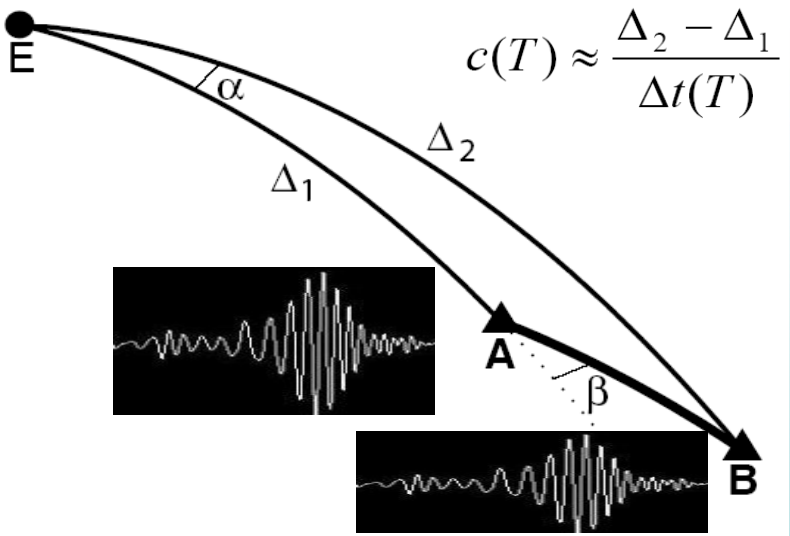

$$c(T) \approx \frac{\Delta_2 - \Delta_1}{\Delta t(T)}$$

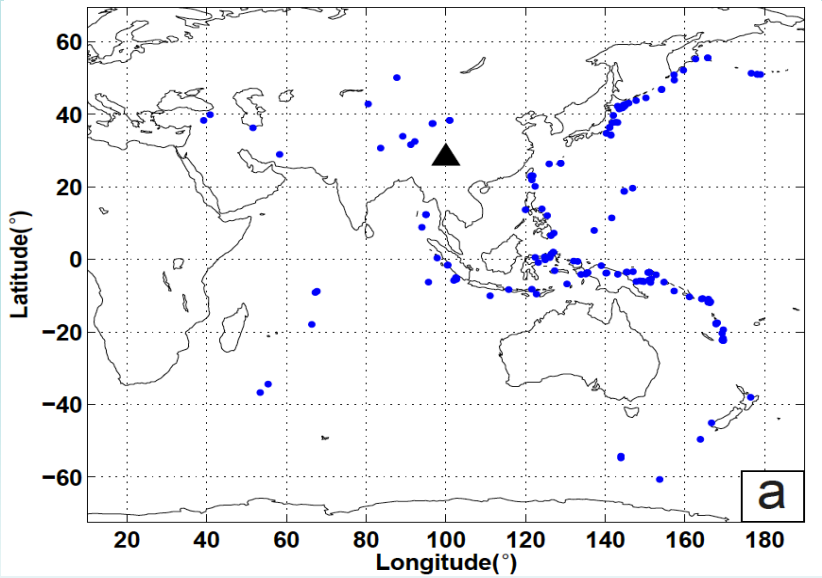

Teleseismic surface waves

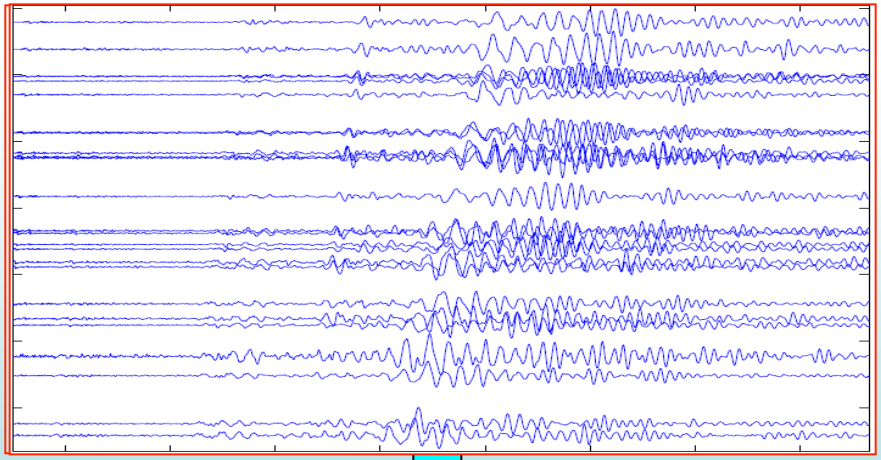

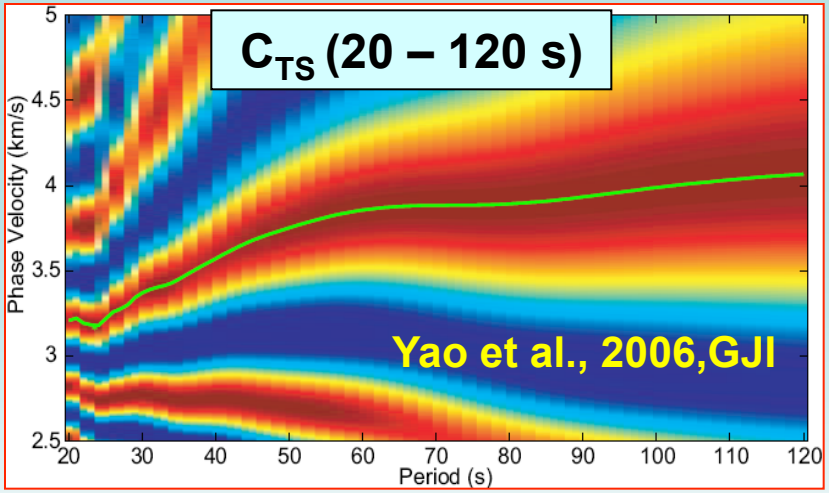

Advantages of phase velocity measurements from ambient noise EGFs

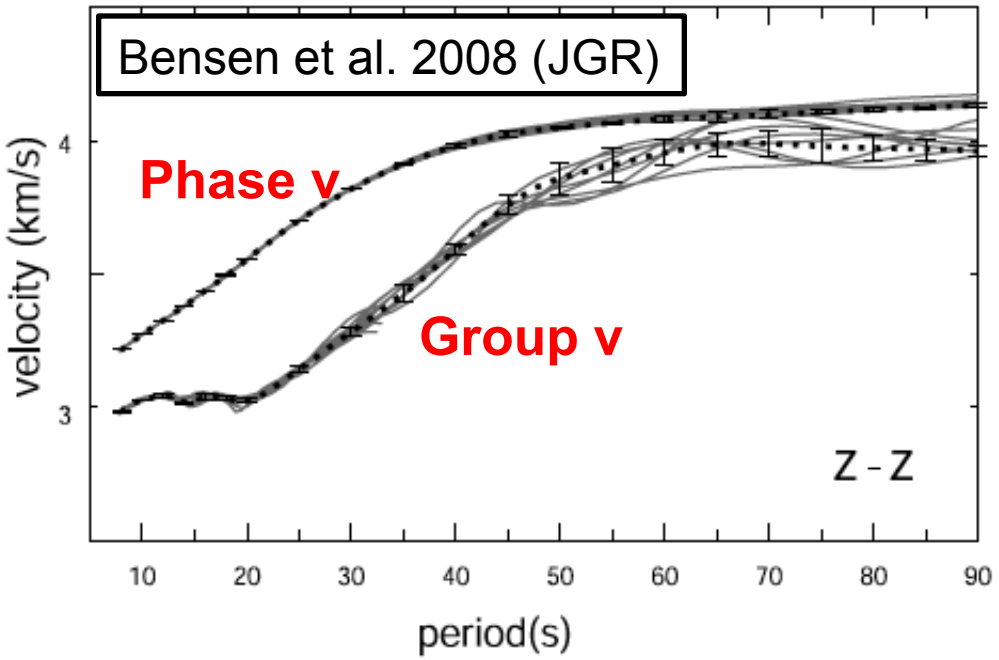

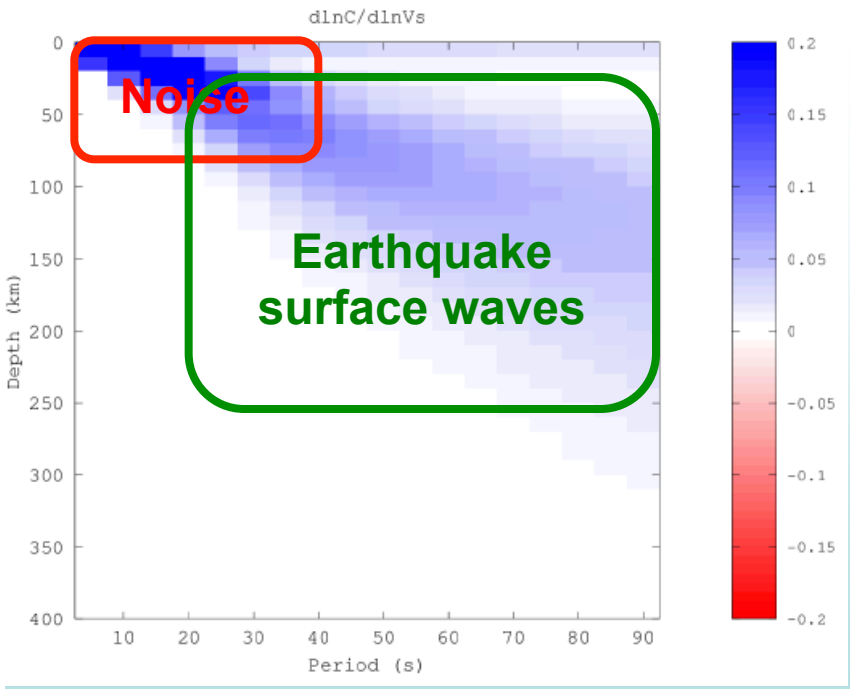

1. Better accuracy at longer periods
(e.g., T=30s ： error in group v ～ 2 x error in phase v)
2. Easy to combine with inter-station phase velocity dispersion from earthquake data
   ambient noise：5—40 s （5—70 km）
   earthquake surface wave：20—150 s （20—250 km）

Sensitivity Kernels of TS and GF based travel times

Yao, van der Hilst, Montagner (2010, JGR)

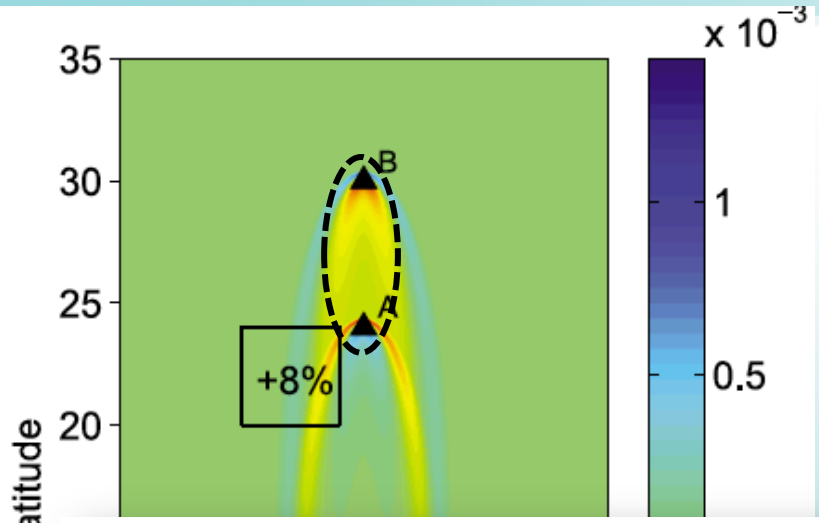

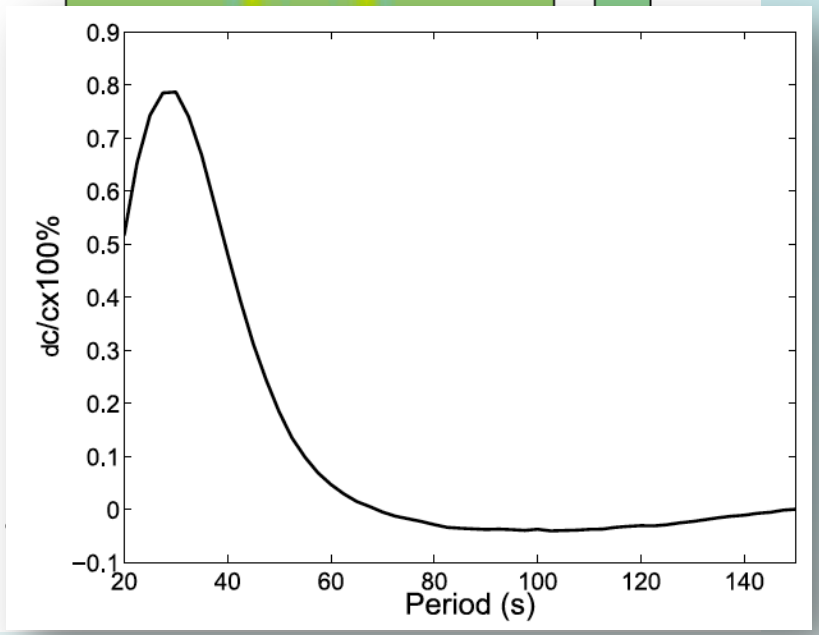

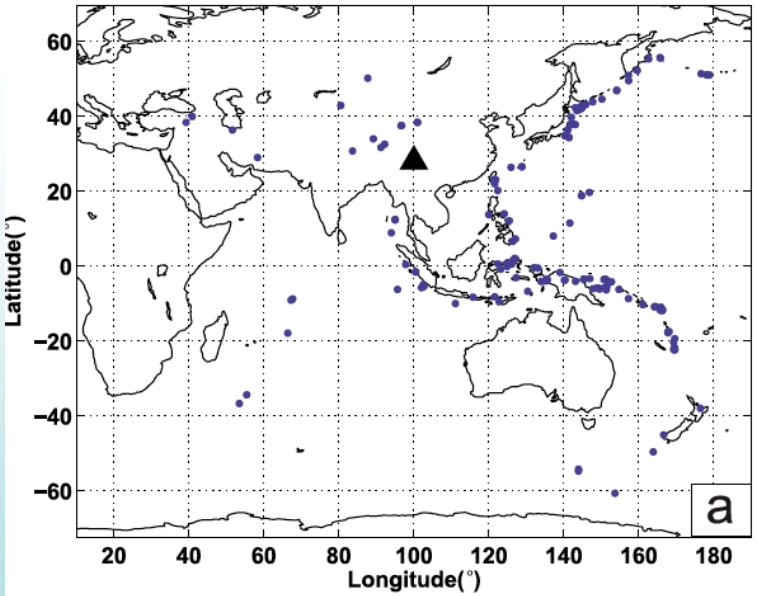

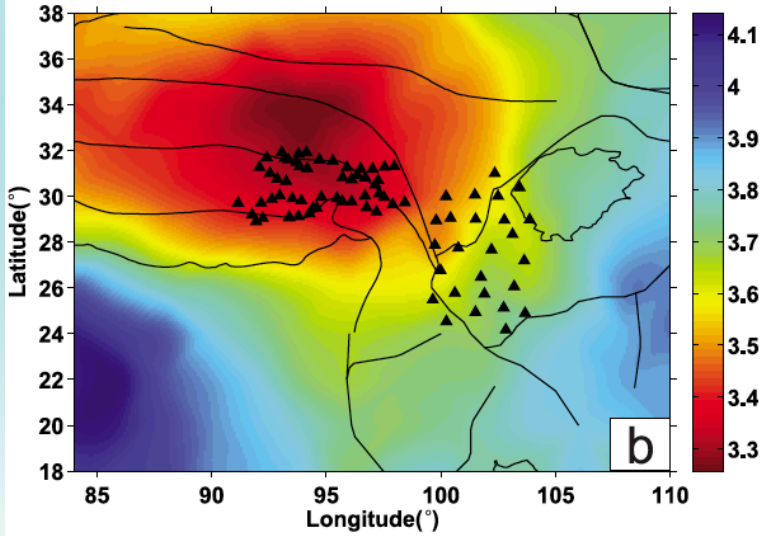

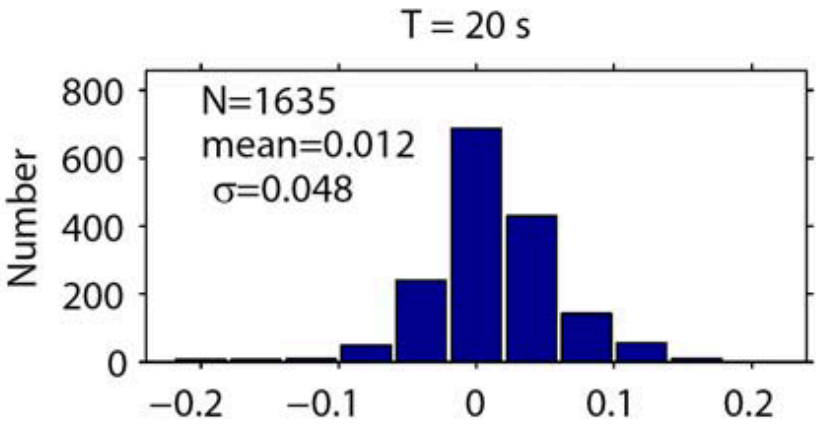

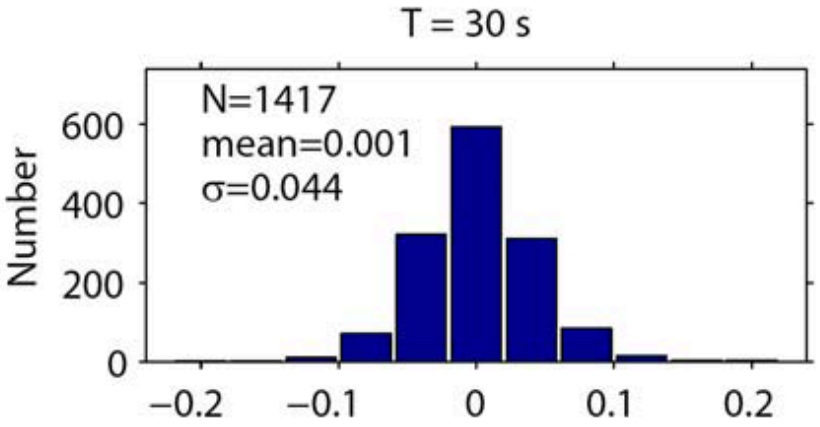

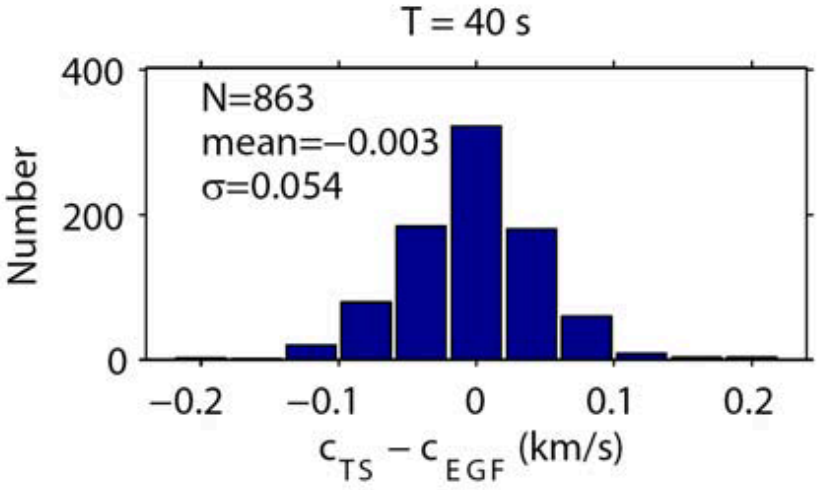

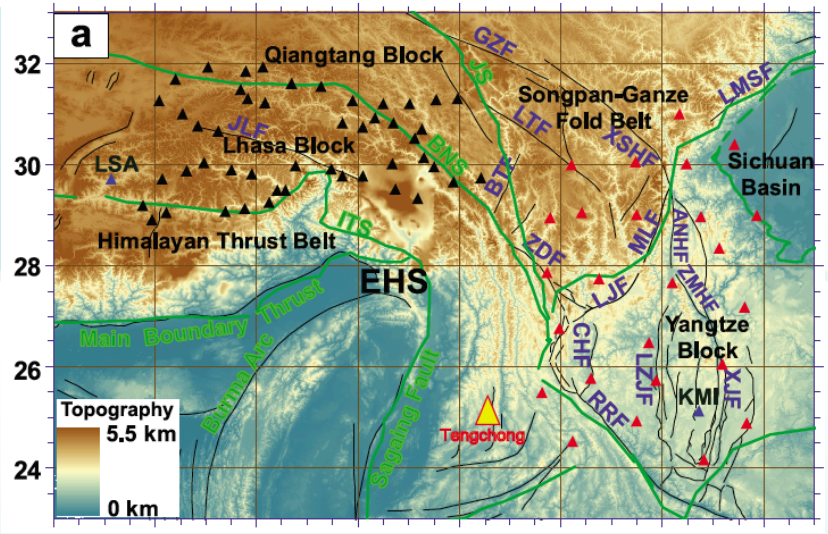

Phase velocity comparison between EGF and TS methods

Similar in the overlapping periods (20-40 s)

For T > 40 s, their differences become much larger

Yao, van der Hilst, Montagner (2010, JGR)

Joint ambient noise and earthquake surface wave tomography: approach 1

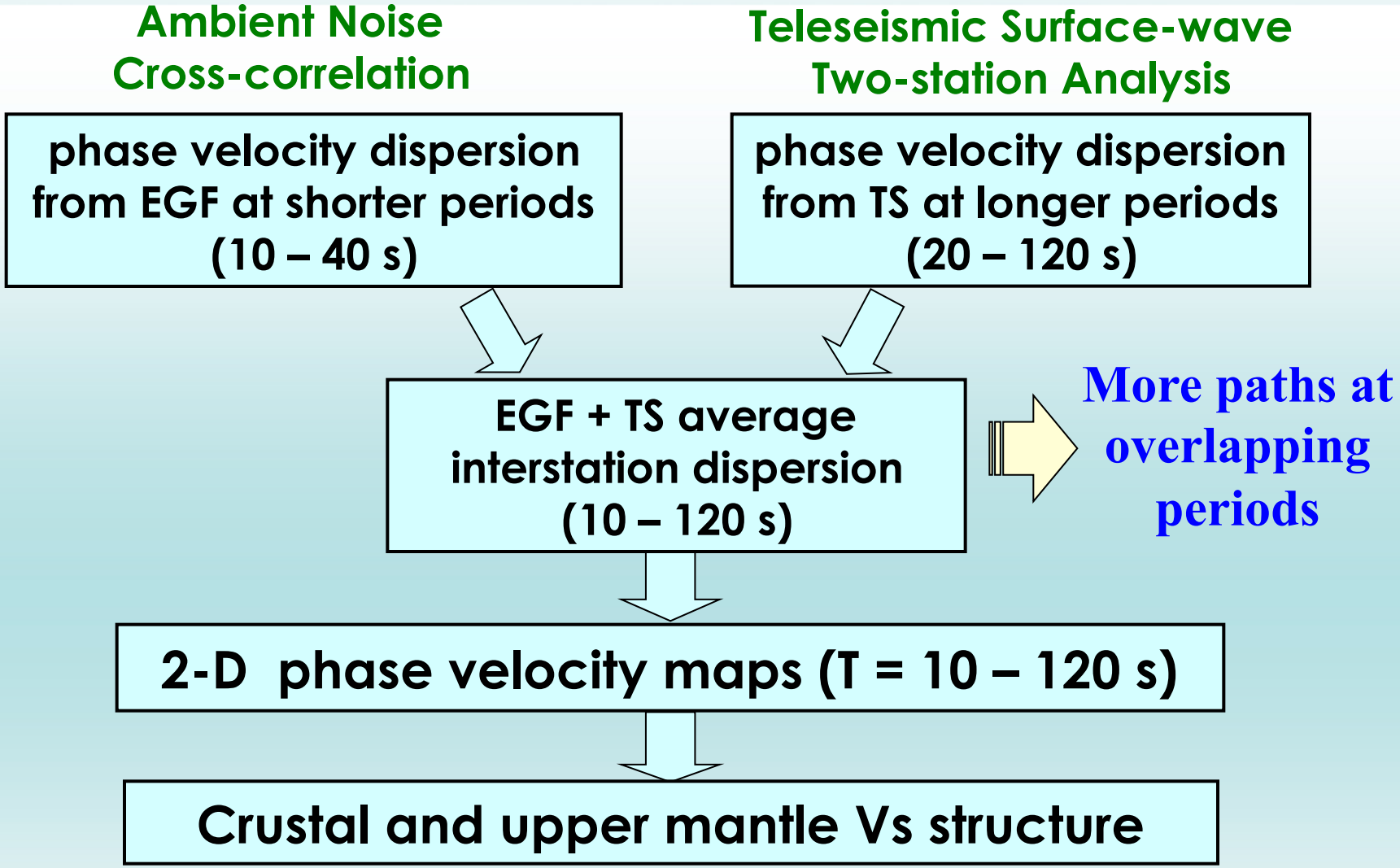

Yao, Beghein, van der Hilst (2008,GJI)

Joint ambient noise and earthquake surface wave tomography: approach 2

Ambient Noise Interferometry

phase velocity dispersion from EGF at shorter periods (5 – 40 s)

Travel time or eikonal tomography

phase velocity maps at shorter periods (~ 5 – 40 s)

Teleseismic Surface-wave two plane-wave method /Helmholtz tomography

phase velocity maps at longer periods (> 40 s)

Crustal and upper mantle Vs structure

(Yingjie Yang et al., 2008, GJI; Fan-Chi Lin et al.)

Uneven noise source distribution and biases in CFs/EGFs

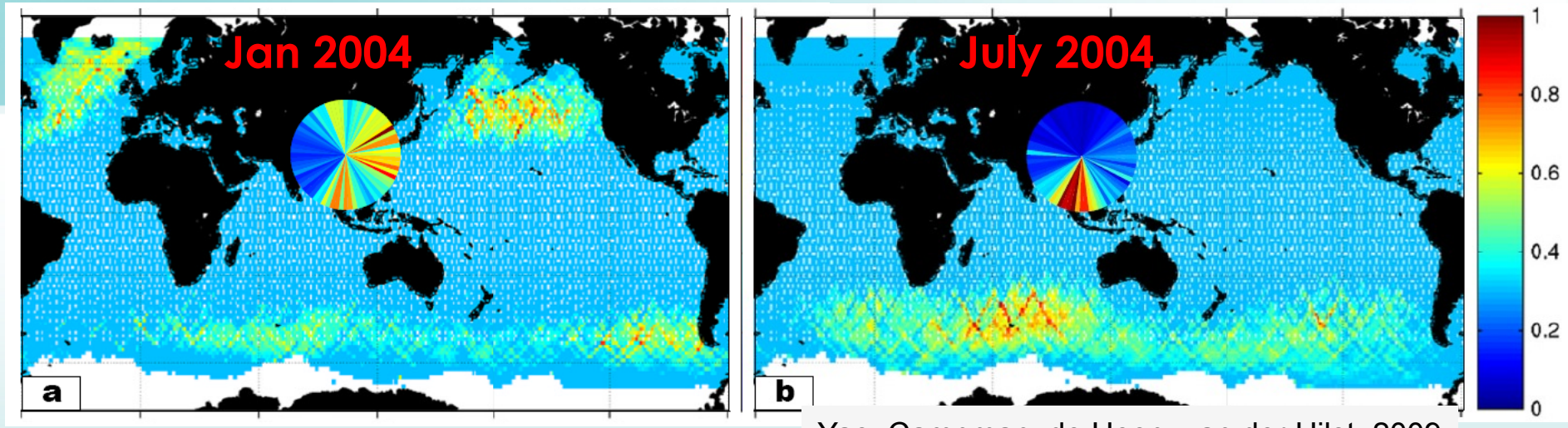

Yao, Campman, de Hoop, van der Hilst, 2009

- **Correlation of ambient noise energy (10-20s) with ocean wave activity** (background image: normalized global ocean wave height in winter time (a) and in summer time (b))

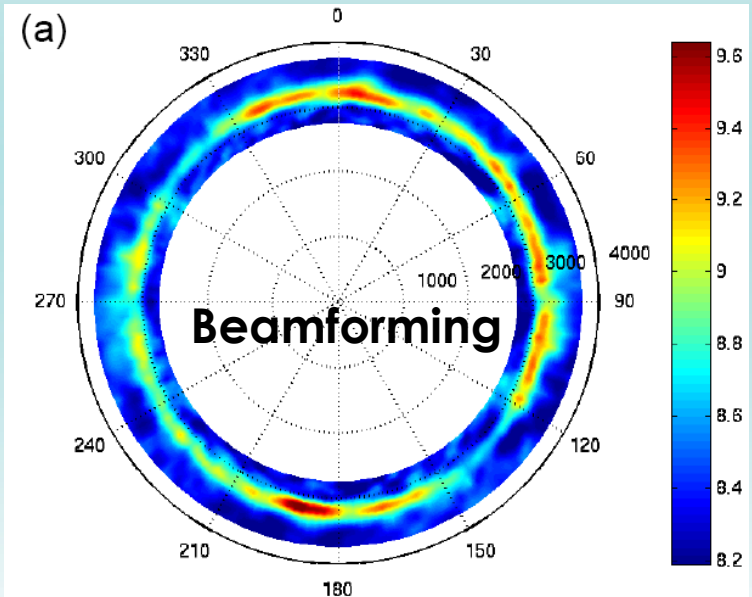

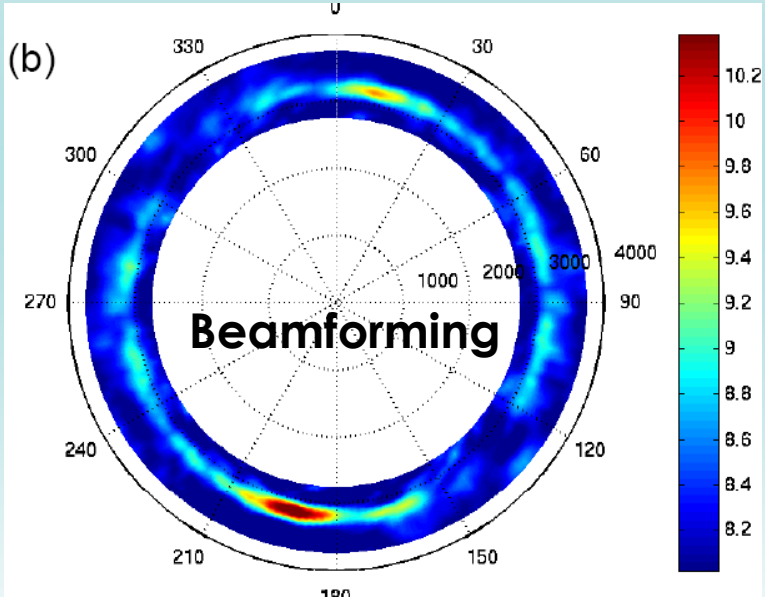

Uneven noise source distribution and its effects on ambient noise tomography

Theoretical works by: Weaver et al. 2009; Tsai, 2009

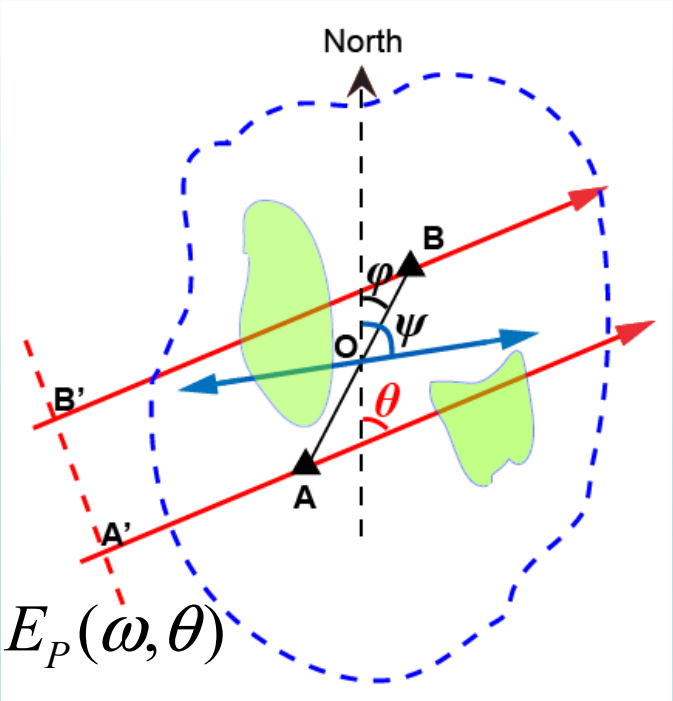

(Yao & van der Hilst, 2009, GJI)

- We use **plane-wave modeling** to estimate the noise energy distribution and phase velocity bias

$$C_{AB}(\omega,t)=\int_0^{2\pi} E_P(\omega,\theta)\cos\left[\omega(t-\delta t)\right]H(t,\delta t)\mathrm{d}\theta$$

δt: based on real model (with azimuthal anisotropy)

Some assumptions:

Small array (plane geometry)

Good inter-station azimuthal coverage

Ambient noise sources are far away

Weak local scattering

Iterative modeling, inversion of noise amplitudes, correction of phase biases and tomographic images

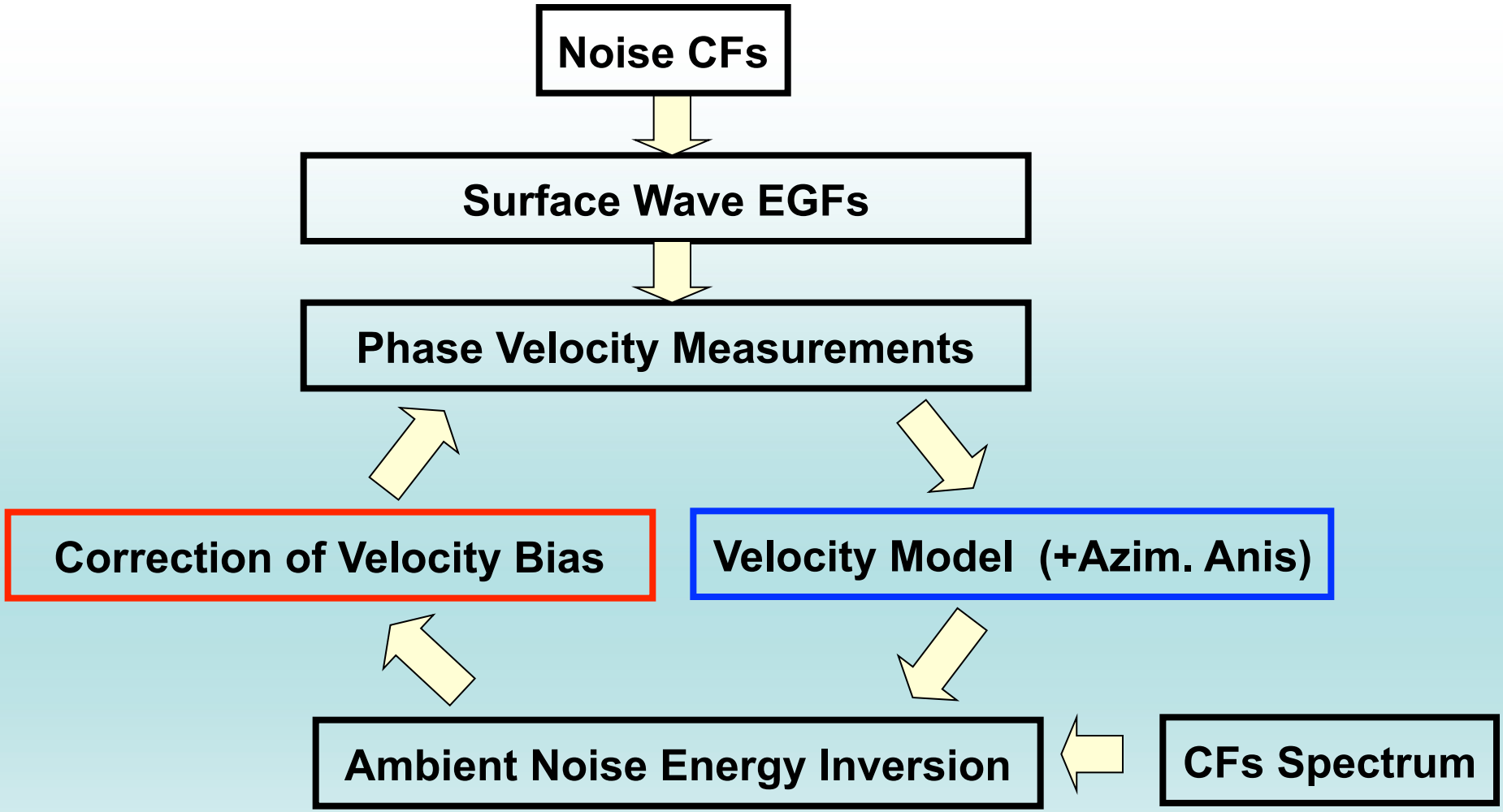

(Yao & van der Hilst, 2009, GJI)

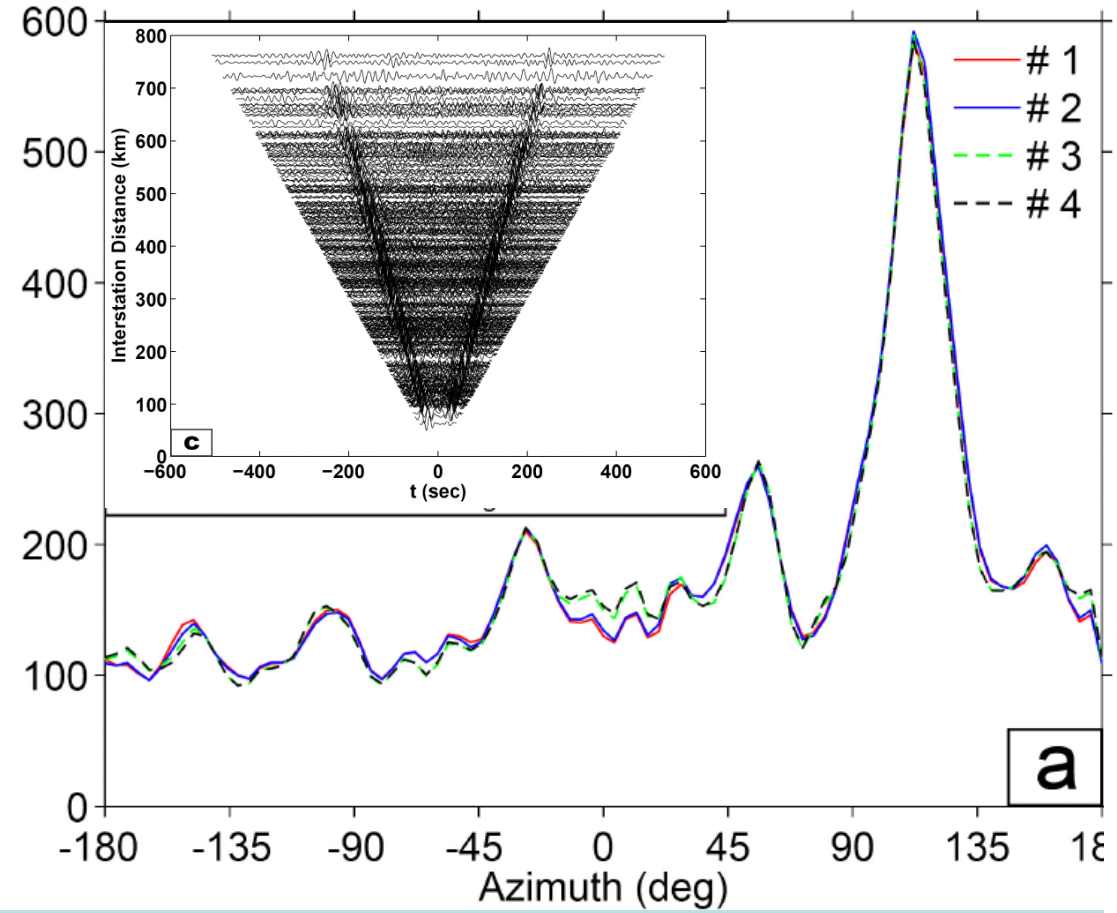

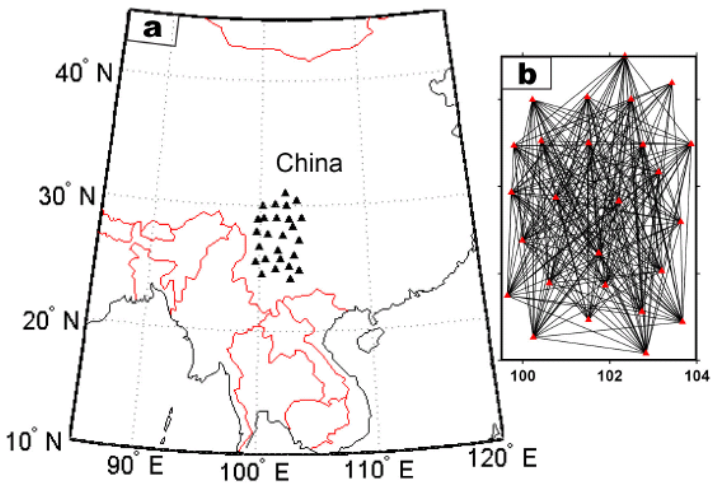

Inversion results of ambient noise energy distribution at T = 25 s

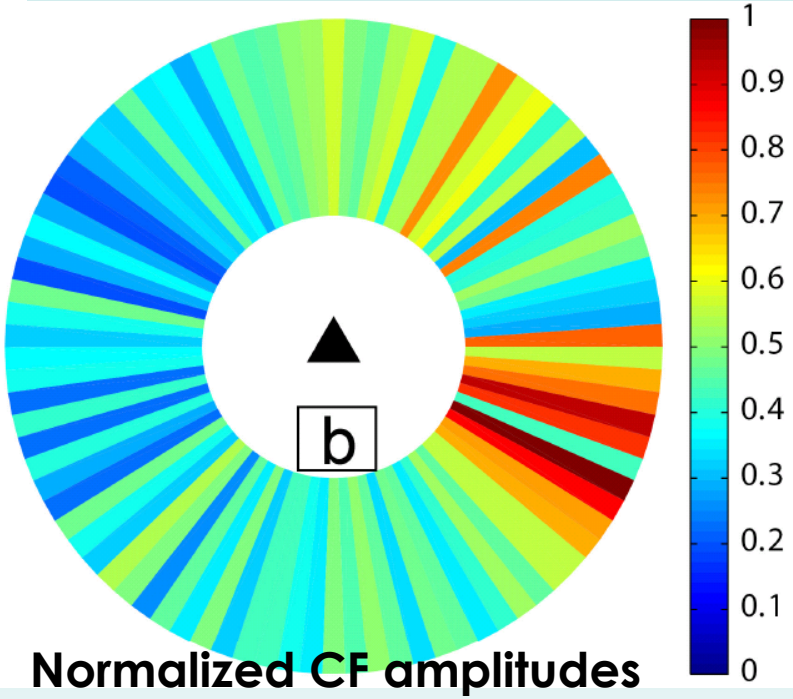

Inter-station phase velocity bias of EGFs

(stack of the causal and anti-causal parts for dispersion analysis)

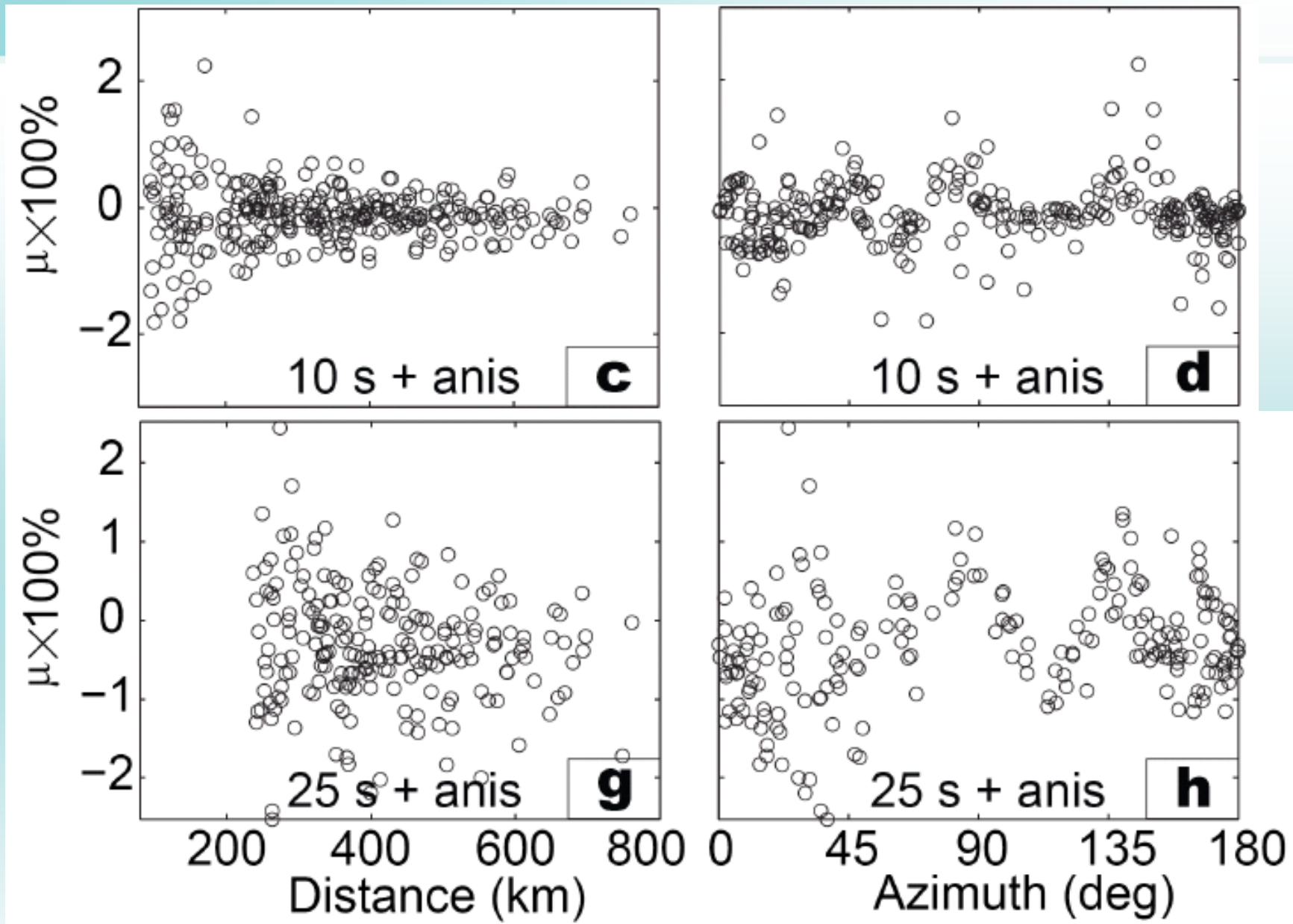

Inter-station phase velocity bias of EGFs

(stack of the causal and anti-causal parts for dispersion analysis)

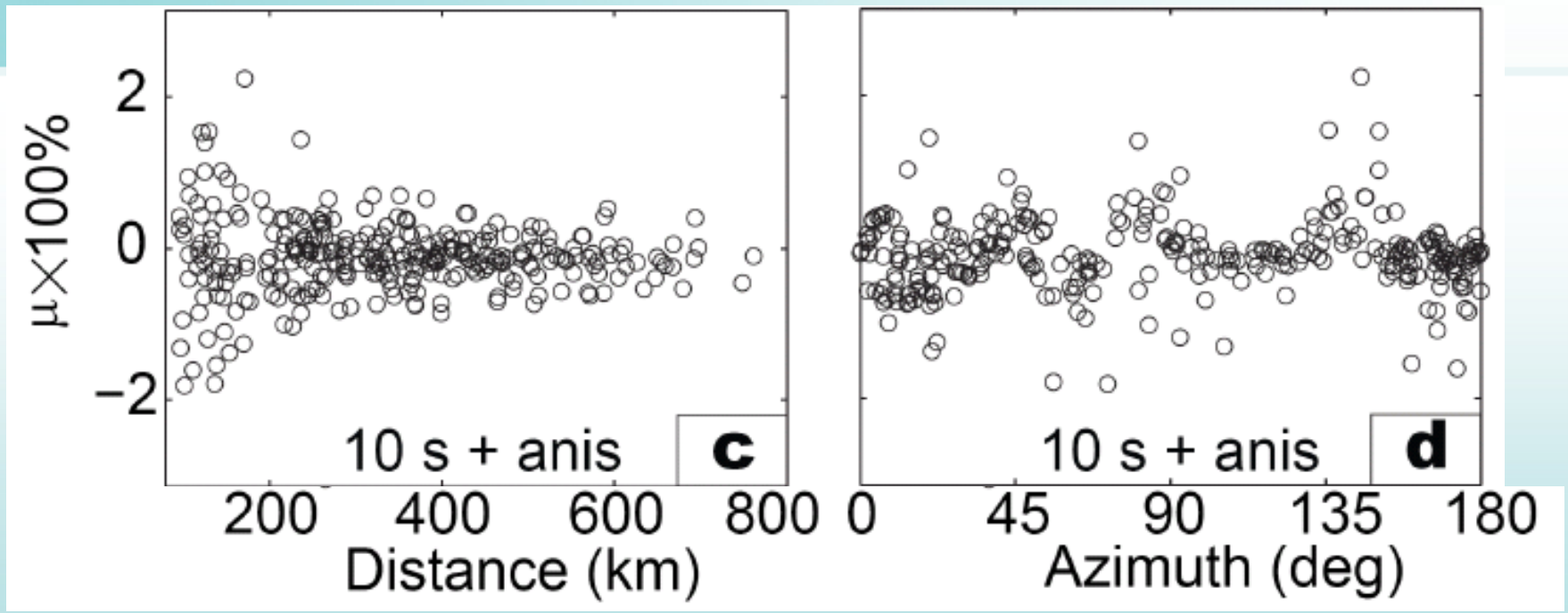

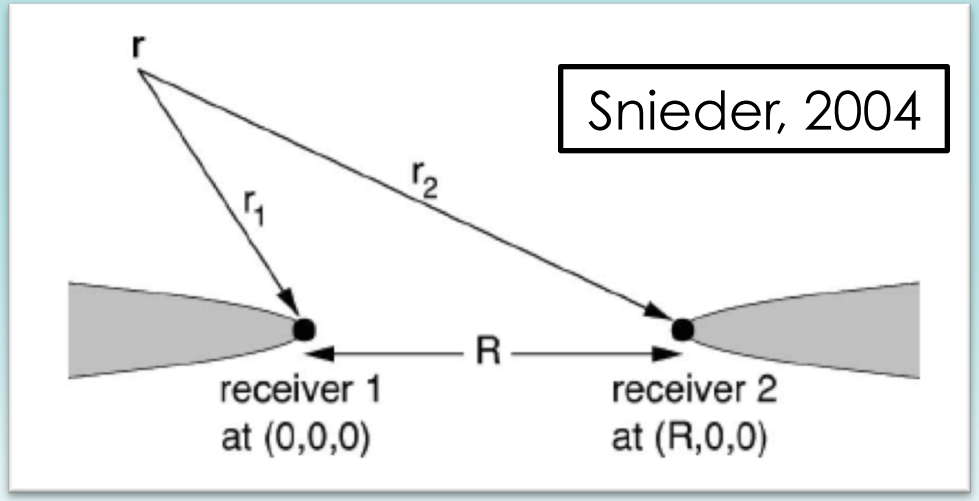

Snieder, 2004

small inter-station distance
or larger wavelength
→ broad influence zone
→ more sensitive to even
source distribution

Before bias correction

After bias correction

10 s

25 s

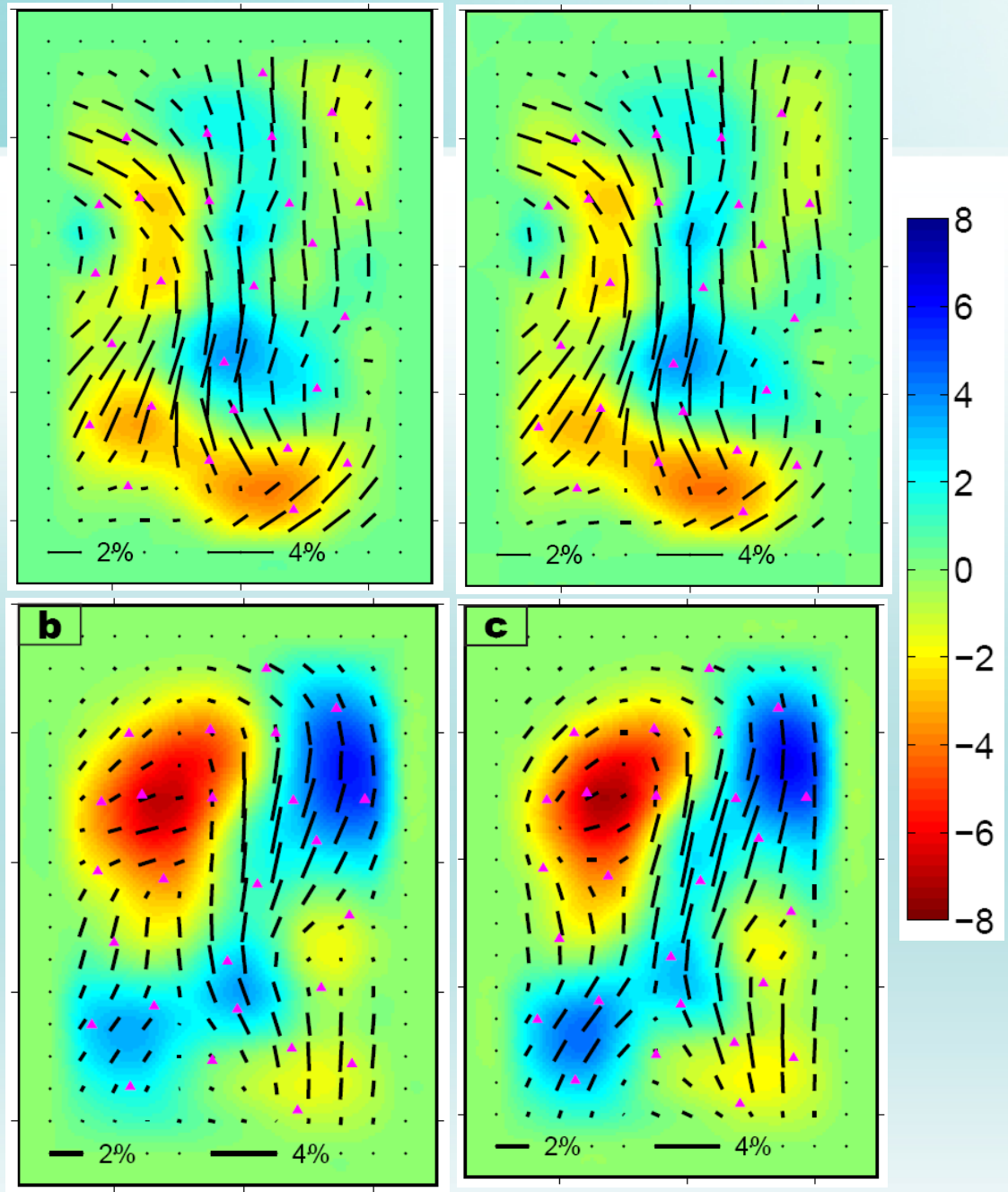

- Effect on phase velocity maps in SE Tibet is very small

reasons:
(1)stack of causal & acausal part EGF for dispersion

(2) Spatial smoothing in the inversion of phase velocity maps

Yao & Van der Hilst (2009)

Outline

- Joint ambient noise and earthquake surface wave tomography (isotropic and anisotropic crust and upper mantle structures)

- **Direct ambient noise/surface wave travel time tomography with ray tracing and wavelet-based inversion**

- Joint ambient noise and body wave travel time tomography

Ambient Noise Tomography: large scale

Great success in global/regional seismology for studying crustal structure (isotropic velocity + radial and azimuthal anisotropy)

→ Standard array technique like receiver function, shear wave splitting, etc

yearly data cross-correlation

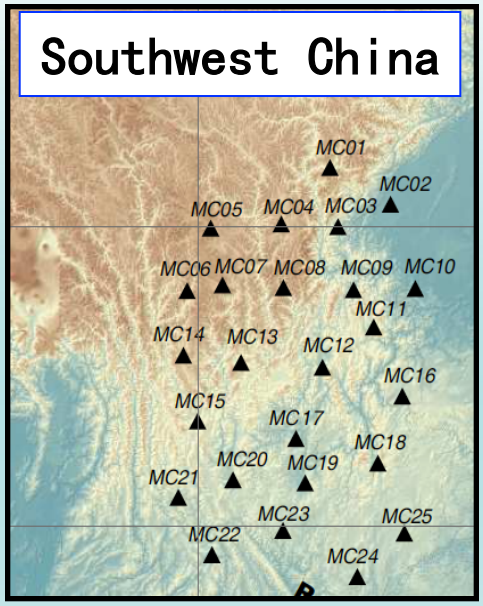

~ 600 km scale

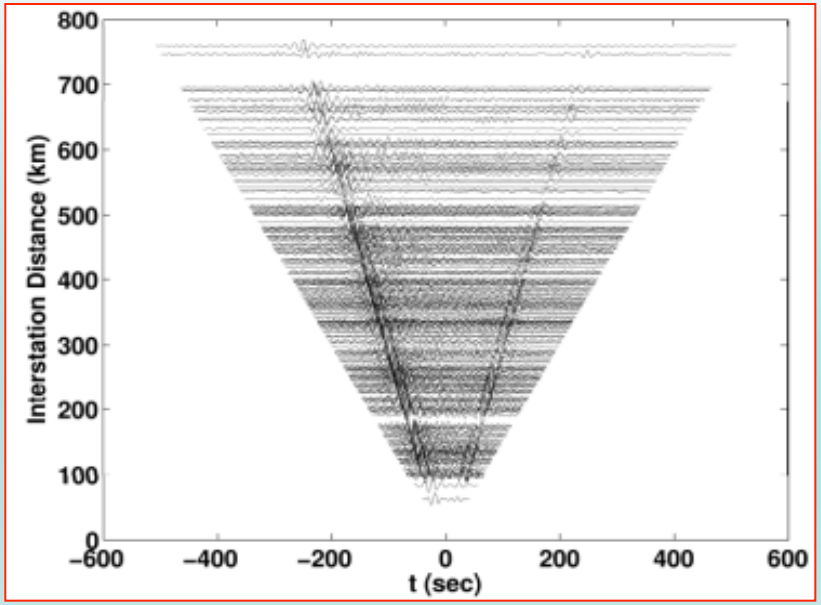

Period: 10 – 40 s

λ: 30 – 150 km

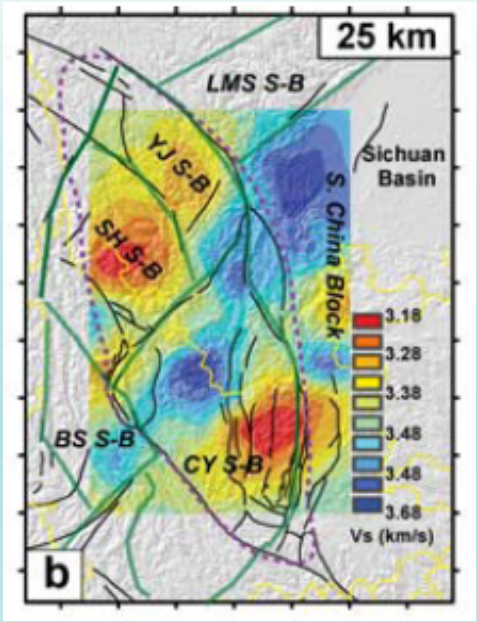

Mid-crust Vs

Yao et al. (2006, 2008)

Ambient Noise Tomography: small scale

Ambient noise tomography can be used to study (very) small scale shear velocity structure with closely spaced receivers.

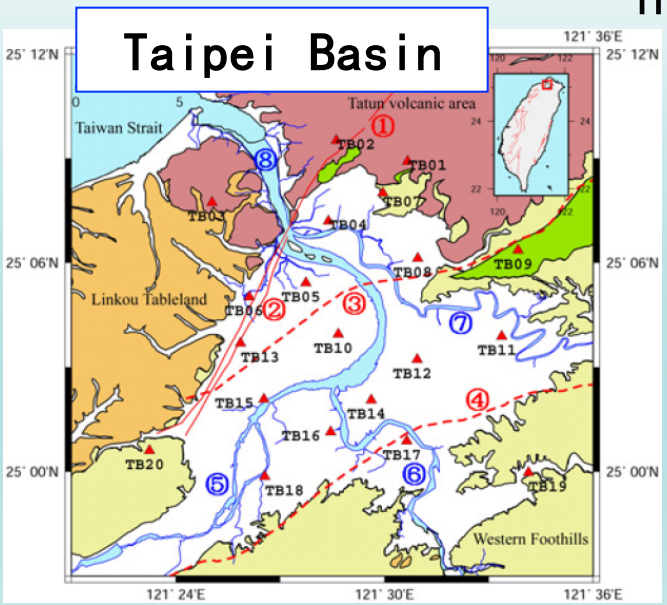

~ 10 km scale

monthly data cross-correlation

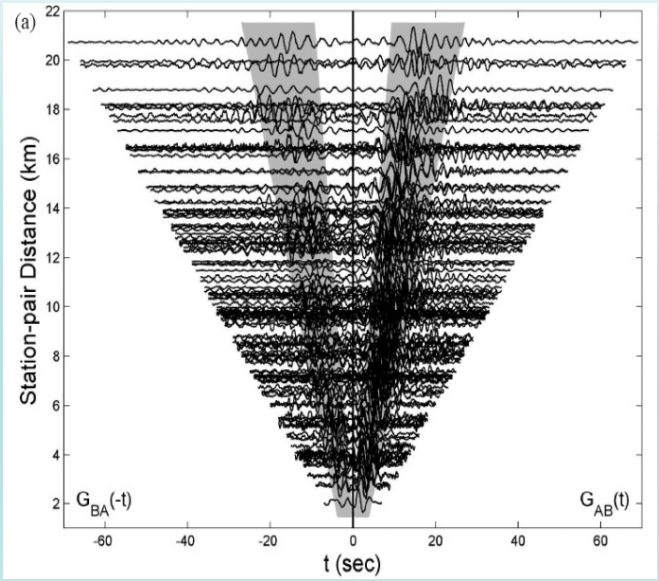

Period: 0.5-2 s
λ: 0.5 – 5 km

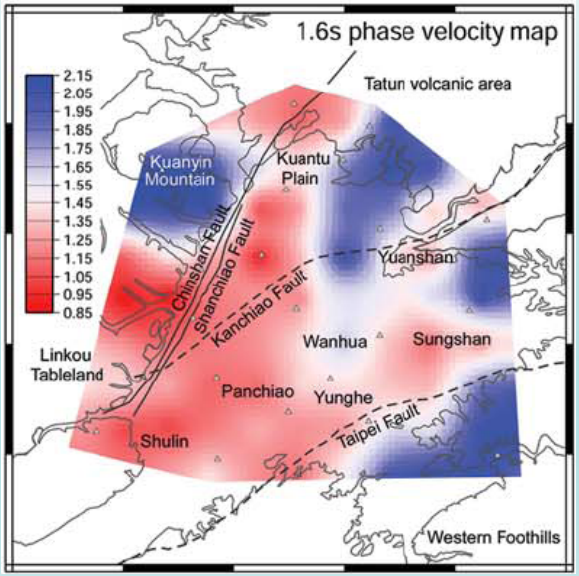

1.6 s phase v map
(shallow upper crust)

Huang, Yao et al. (2010)

Shallow crustal / near surface structure

- Important for estimation of strong ground motion due to earthquakes
- Important for characterizing structures of oil/gas reservoir and mineral deposit fields

Most studies use either active sources or local earthquakes to image near surface structure

Ambient noise tomography provides an alternative and inexpensive way for imaging near surface structure

Ambient noise tomography for shear velocity structure

Traditional methods

NCFs or EGFs

↓

Path-dependent surface wave dispersion data

↓ **Traveltime tomography**

2D phase/group velocity maps

↓ **Pointwise 1-D inversion**

3D shear velocity structure

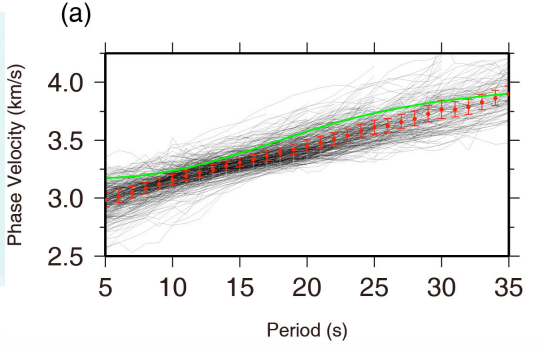

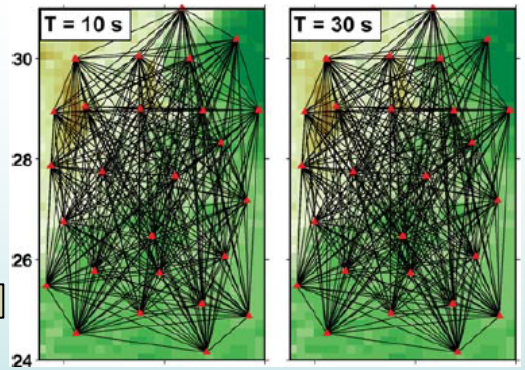

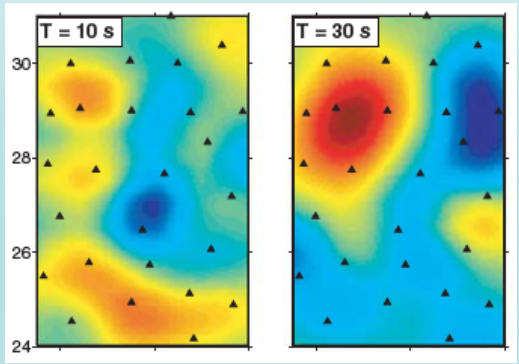

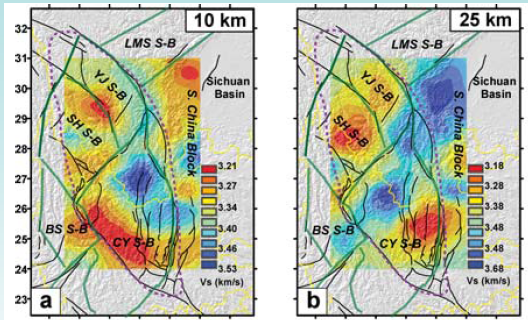

Ambient noise tomography for shear velocity structure

Eikonal tomography (Lin et al. 2009)

NCFs or EGFs

Dense array receiver-receivers surface wave traveltime data

$$\frac{\hat{k}_i}{c_i(r)} \cong \nabla\tau(r_i, r)$$

Eikonal tomography

2D phase velocity maps

Pointwise 1-D inversion

3D shear velocity structure

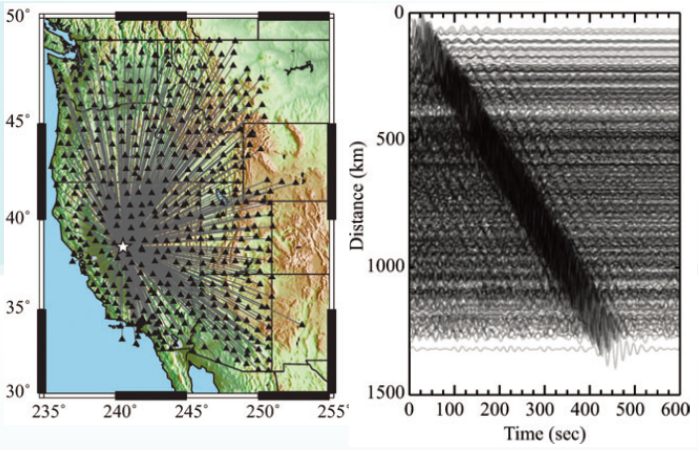

t surface

estimated c

T = 24 s

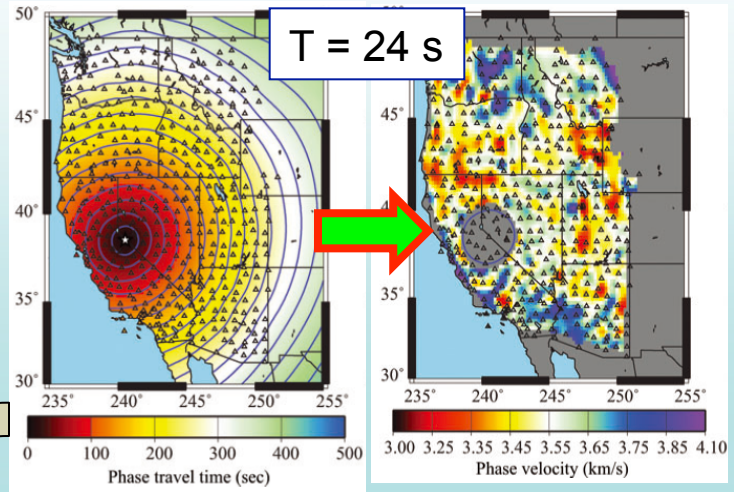

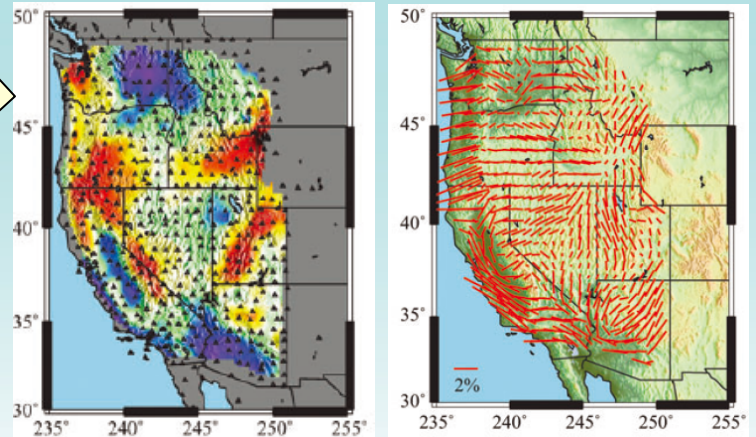

Resolution issues

Eikonal: straightforward method, no inversion, good estimation of azimuthal anisotropy

Spatial smoothing of traveltime surface → stable phase velocity maps, but lower spatial resolution (<station spacing) compared to traveltime tomography

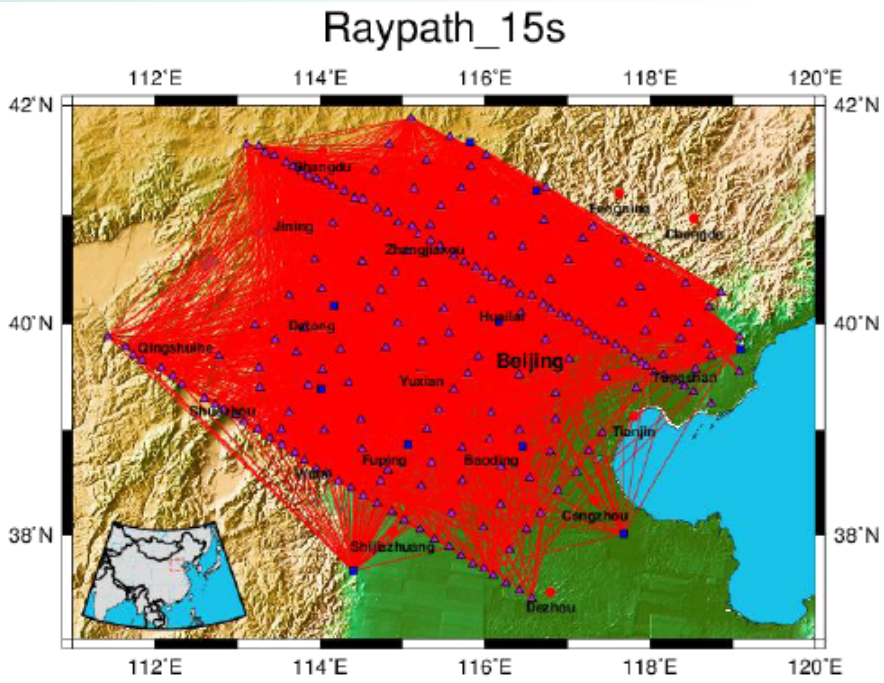

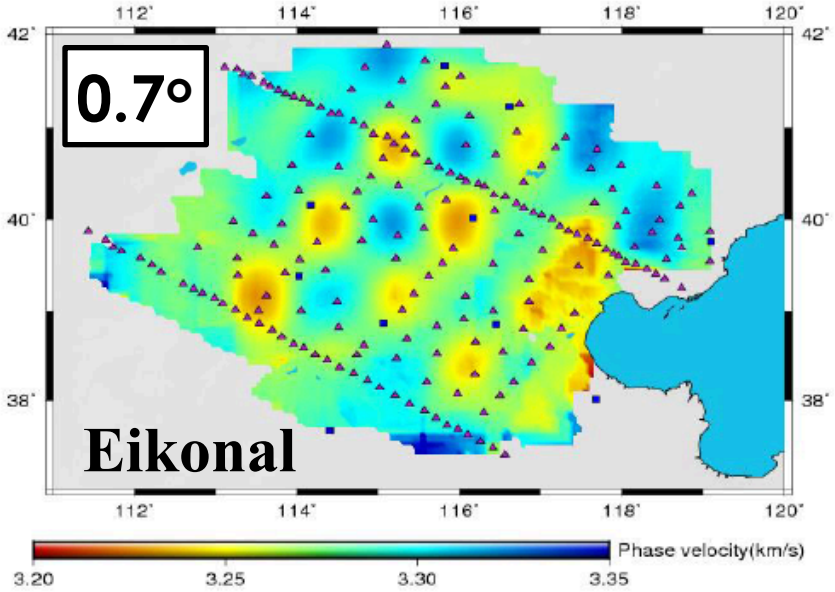

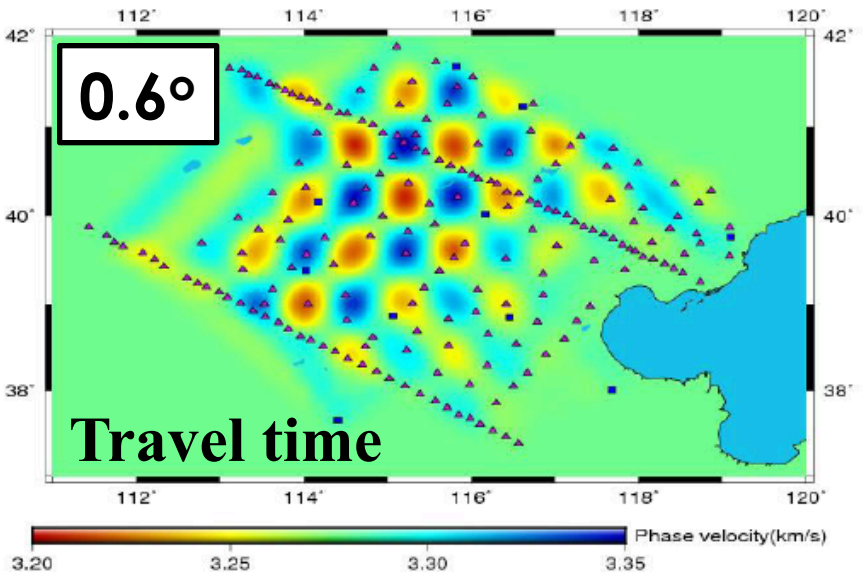

Active source Eikonal tomography: dense array in reservoir scale

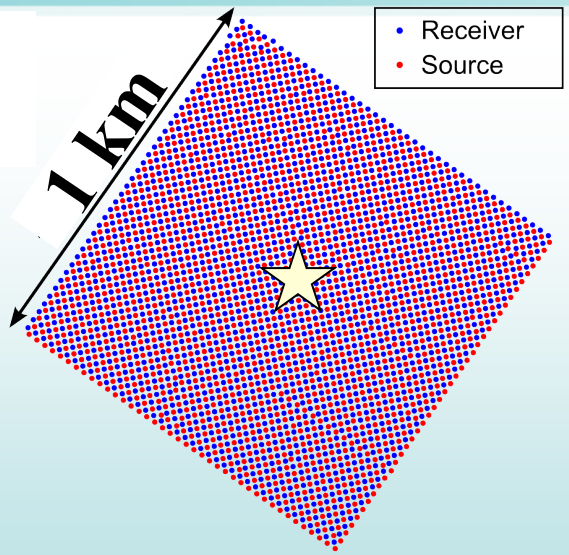

Active source data: a shot gather

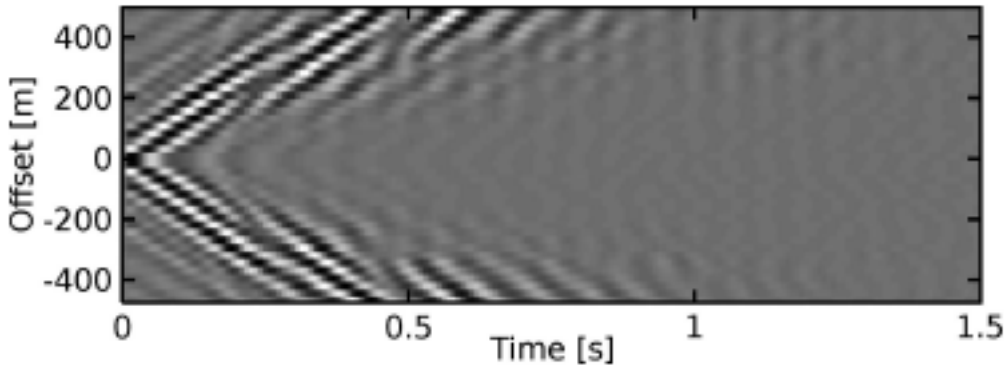

Neighborhood-based cross-correlation method to measure traveltimes

→ to void high-freq cycle skipping problem

$$\mathbf{D}\, t^s = \Delta t^s$$

t^s : receiver traveltime vector

Δt^s : differential traveltimes between neighboring receivers

D: difference operator (matrix)

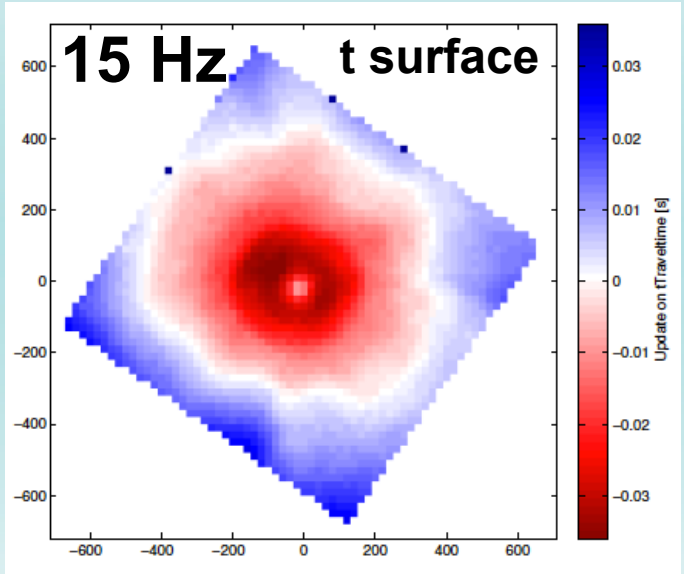

Gouedard, Yao, et al., 2012, GJI

Active source Eikonal tomography

10 Hz

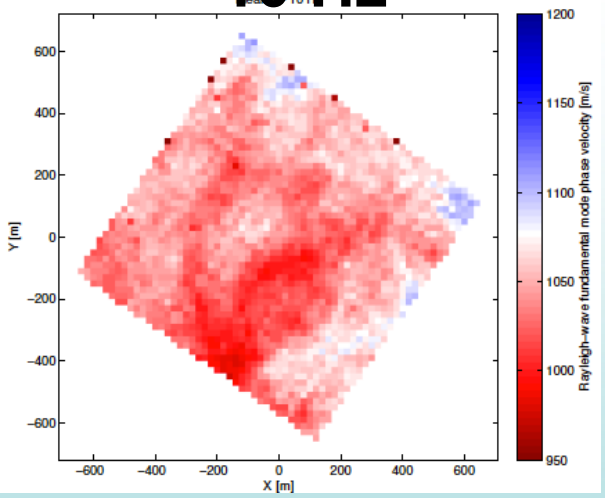

15 Hz

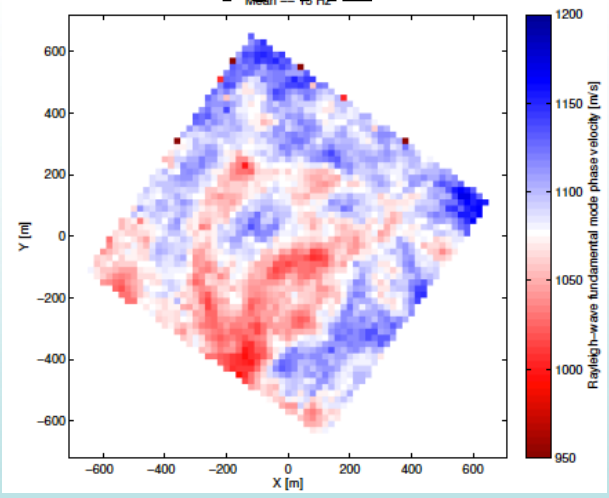

20 Hz

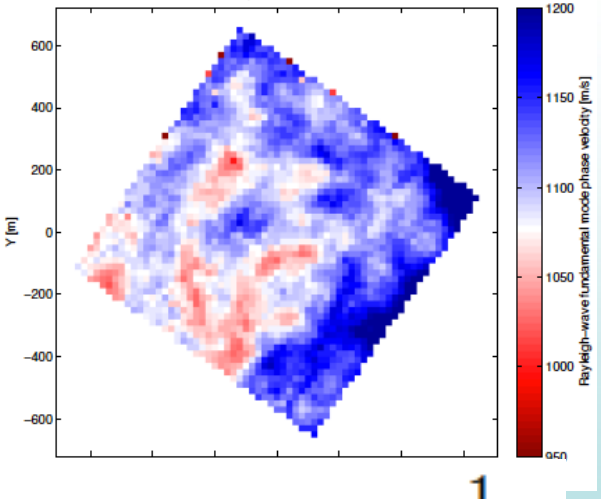

$$|\nabla t(\mathbf{r}_s, \mathbf{r})|^2 \approx \frac{1}{\hat{c}_s^2(\mathbf{r})}$$

Geophysical Journal International

Geophys. J. Int. (2012)

doi: 10.1111/j.1365-246X.2012.05652.x

Surface wave eikonal tomography in heterogeneous media using exploration data

Pierre Gouédard,[1] Huajian Yao,[1,2] Fabian Ernst[3] and Robert D. van der Hilst[1]

Active source Eikonal tomography

15 Hz

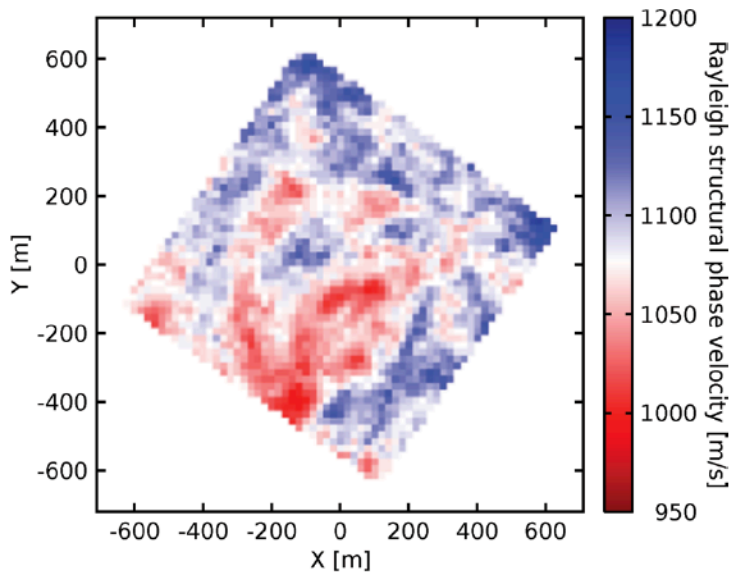

Average over 1600 sources

How many sources to average?

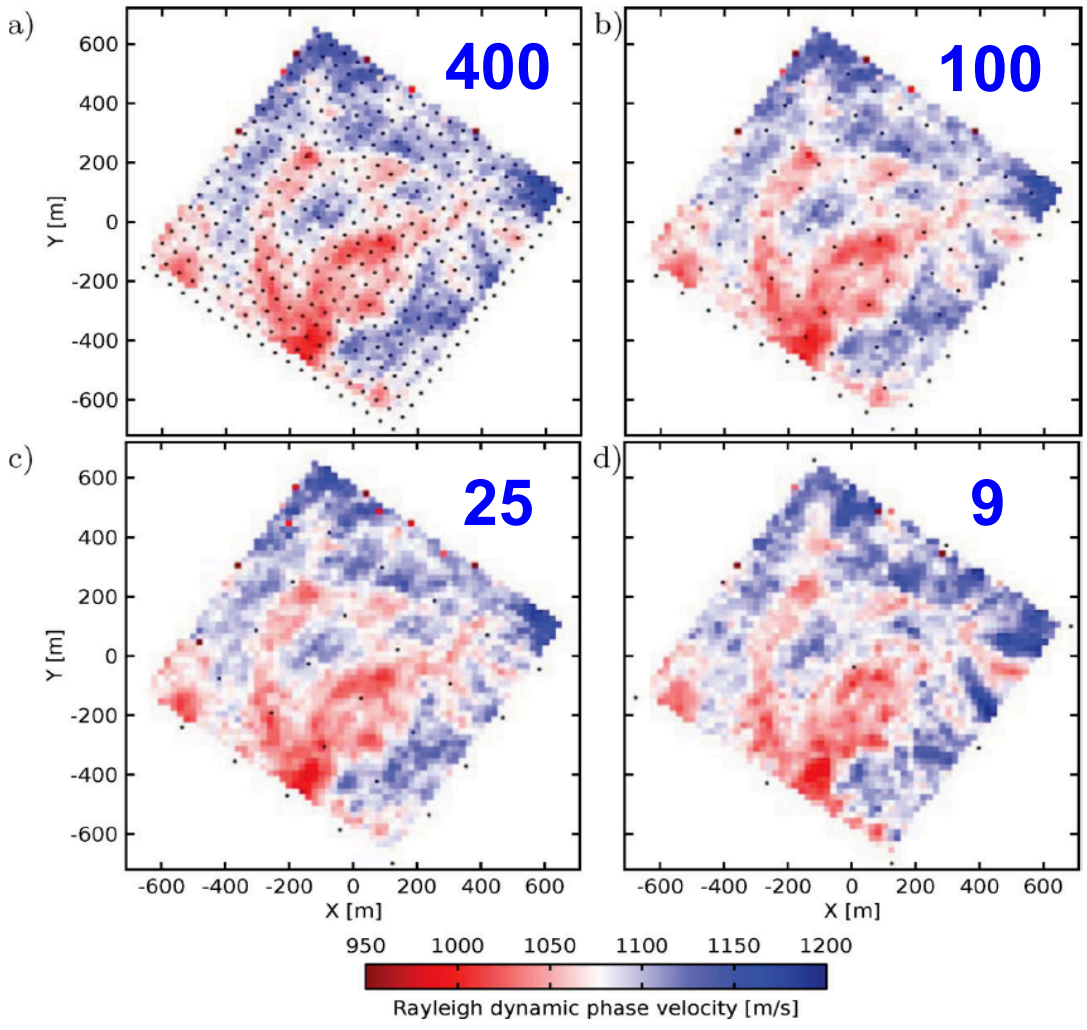

Ambient noise tomography for shear velocity structure

Direct inversion method

NCFs or EGFs

↓

Path-dependent surface wave dispersion data

Boschi & Ekström (2002): global surface wave tomography (no update on ray paths)

↓

3D shear velocity structure

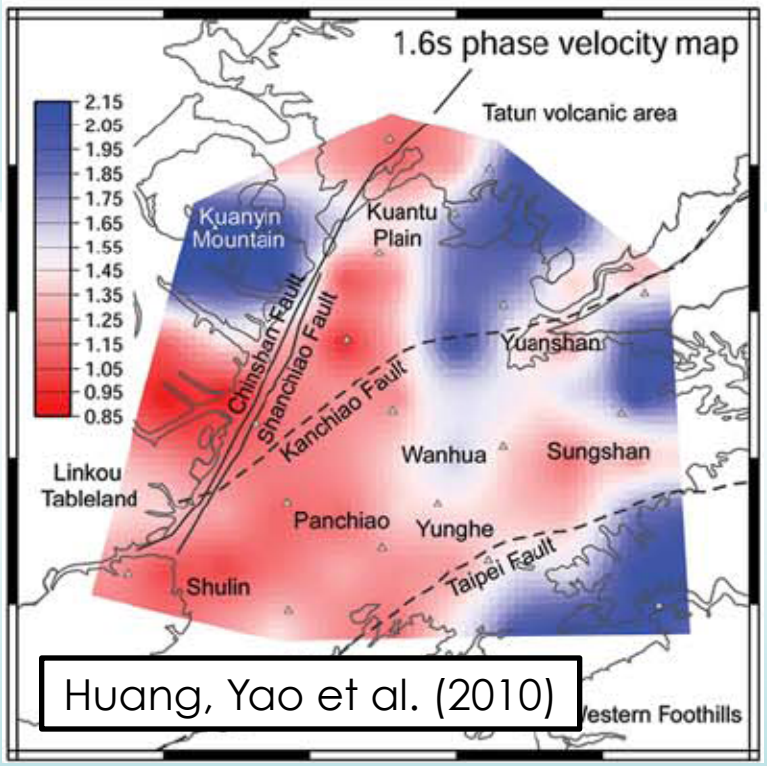

Phase Velocity perturbation > 30%

Need to consider frequency-dependent off-great-circle propagation effect: surface wave raytracing using fast marching method (Rawlinson, 2004)

Direct ambient noise / surface wave tomography for 3-D Vs structure with ray tracing

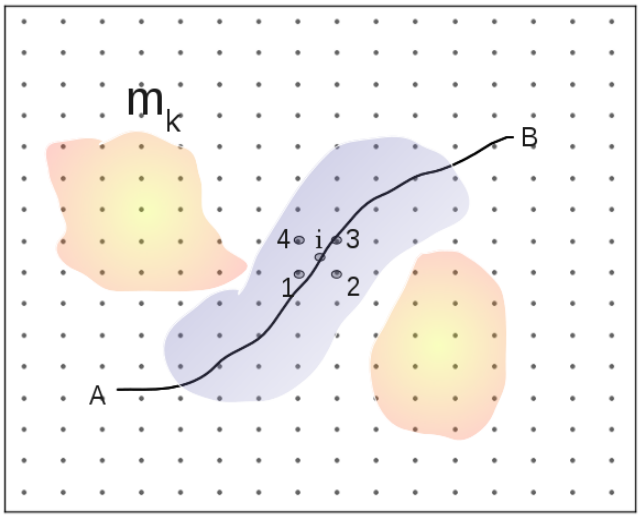

Traveltime at freq. ω :

Slowness along path

$$t_{AB} = \int_A^B S(l_{AB}, w)dl = \sum_{p=1}^{P} S_p(l_{AB}, w)\Delta l_{AB},$$

$$S_p(l_{AB}, w) = \sum_{k=1}^{K} \nu_{pk}\hat{S}_k(w),$$

Slowness at grids

$$t_i(w) = \sum_{k=1}^{K} \upsilon_{ik}\hat{S}_k(w),$$

Traveltime perturbation:

$$\delta t_i(w) = t_i(w) - t_i^r(w) = \sum_{k=1}^{K} \upsilon_{ik}\delta\hat{S}_k(w) = -\sum_{k=1}^{K} \upsilon_{ik}\frac{\delta C_k(w)}{C_k^2(w)},$$

Ref. travel time

Direct ambient noise / surface wave tomography for 3-D Vs structure with ray tracing

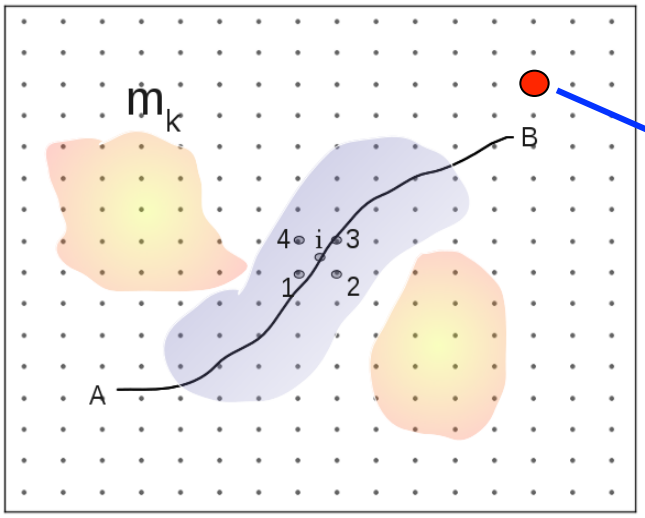

Local 1-D model

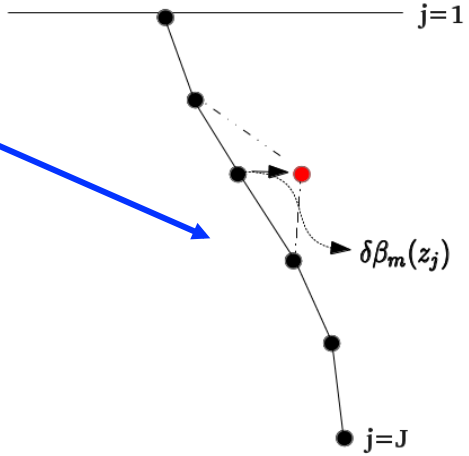

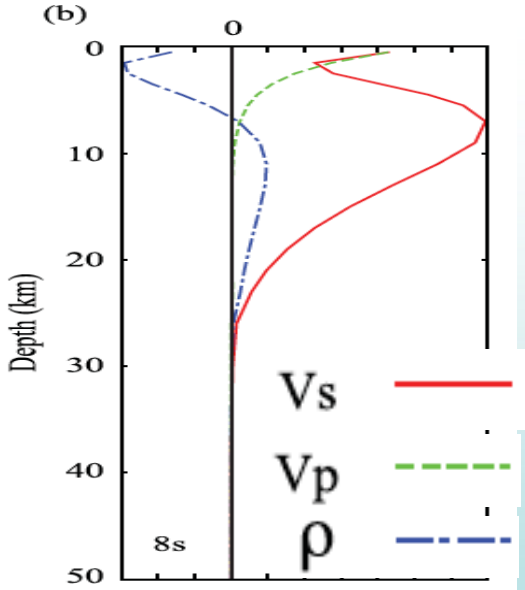

Lin et al. 2014 GJI

$$\delta C_k(w) = \int \left[\left.\frac{\partial C_k(w)}{\partial \alpha_k(z)}\right|_{M^r} \delta\alpha_m(z) + \left.\frac{\partial C_k(w)}{\partial \beta_k(z)}\right|_{M^r} \delta\beta_k(z) + \left.\frac{\partial C_k(w)}{\partial \rho_k(z)}\right|_{M^r} \delta\rho_k(z) \right] dz,$$

Short period Rayleigh waves : also large sensitivity to shallow crustal Vp & density structure

Direct ambient noise / surface wave tomography for 3-D Vs structure with ray tracing

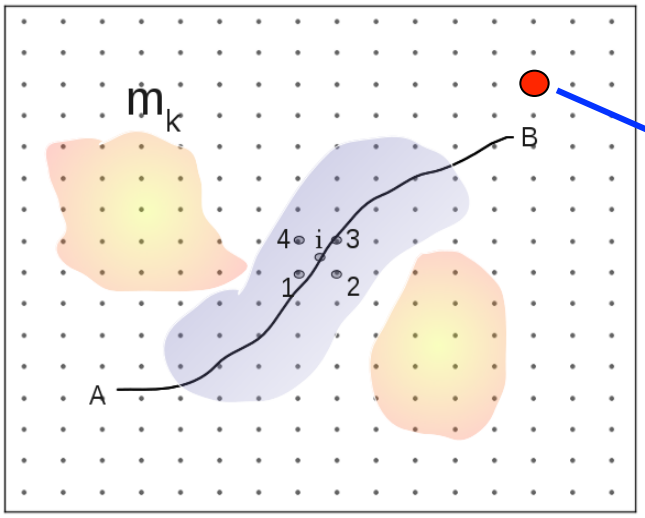

Local 1-D model

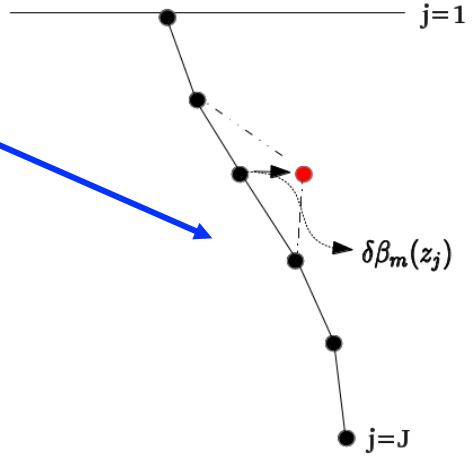

update model → compute 2-D phase v maps → update all ray paths at each f and G matrix iteratively

$$\delta C_k(w) = \int \left[\left.\frac{\partial C_k(w)}{\partial \alpha_k(z)}\right|_{M^r} \delta\alpha_m(z) + \left.\frac{\partial C_k(w)}{\partial \beta_k(z)}\right|_{M^r} \delta\beta_k(z) + \left.\frac{\partial C_k(w)}{\partial \rho_k(z)}\right|_{M^r} \delta\rho_k(z) \right] dz,$$

$$\delta t_i(w) = \sum_{k=1}^{K} \left(-\frac{v_{ik}}{C_k^2}\right) \sum_{j=1}^{J} \left[P'_\alpha(z)\frac{\partial C_k}{\partial \alpha_k(z)} + P'_\rho(z)\frac{\partial C_k}{\partial \rho_k(z)} + \frac{\partial C_k}{\partial \beta_k(z)} \right]\Bigg|_{M^r} \delta\beta_k(z_j) = \sum_{j=1}^{KJ} G_{ij} m_j,$$

$$\Rightarrow \quad \mathbf{d} = \mathbf{G}\mathbf{m}$$

$$\Phi(\mathbf{m}) = \left\|\mathbf{d} - \mathbf{G}\mathbf{m}\right\|_2^2 + \lambda \left\|\mathbf{L}\mathbf{m}\right\|_2^2$$

$$\hat{\mathbf{m}} = \left(\mathbf{G}^T\mathbf{G} + \lambda\mathbf{L}^T\mathbf{L}\right)^{-1}\mathbf{G}^T\mathbf{d}$$

Wavelet-based sparsity-constrained tomography: multiscale resolution based on ray path density

Orthogonal wavelet basis: $\mathbf{W^{-1} = W^{T}}$

Then: $\tilde{\mathbf{m}} = \mathbf{W}\mathbf{m} \quad \tilde{\mathbf{G}} = \mathbf{G}\mathbf{W}^{\mathbf{T}}$

Velocity model is sparse under wavelet basis:

$$min\|\tilde{\mathbf{G}}\tilde{\mathbf{m}} - \mathbf{d}\|_1 + \lambda\|\tilde{\mathbf{m}}\|_1$$

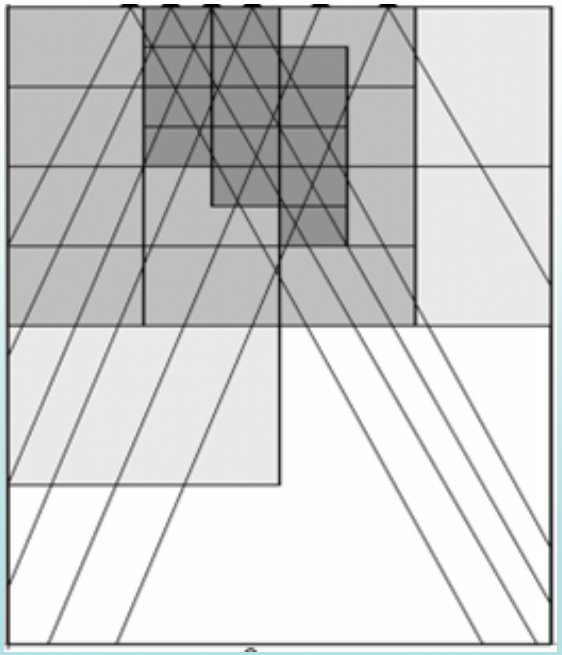

L1 norm of data misfit: more robust to data outliers

L1 norm of model parameters : sparse wavelet coefficients

Solved by Iteratively Reweighted Least Squares Method (IRLS)

Fang, Yao et al., GJI, 2015

Geophysical Journal International

Geophys. J. Int. (2015) **201,** 1251–1263 doi: 10.1093/gji/ggv080

GJI Seismology

Direct inversion of surface wave dispersion for three-dimensional shallow crustal structure based on ray tracing: methodology and application

Hongjian Fang,[1,2] Huajian Yao,[1,2] Haijiang Zhang,[1,2] Yu-Chih Huang[3,4] and Robert D. van der Hilst[5]

[1] *Laboratory of Seismology and Physics of Earth's Interior, School of Earth and Space Sciences, University of Science and Technology of China, Hefei* 230026, *China. E-mail: hjyao@ustc.edu.cn*

[2] *National Geophysical Observatory at Mengcheng, Anhui, China*

[3] *Institute of Earth Sciences, Academia Sinica, Taipei, Taiwan*

[4] *Taiwan Volcano Observatory at Tatun, Ministry of Science and Technology, Taipei, Taiwan*

[5] *Department of Earth, Atmospheric, and Planetary Sciences, Massachusetts Institute of Technology, Cambridge, MA* 02139, *USA*

Examples of direct ambient noise tomography

(1) Taipei Basin in Taiwan

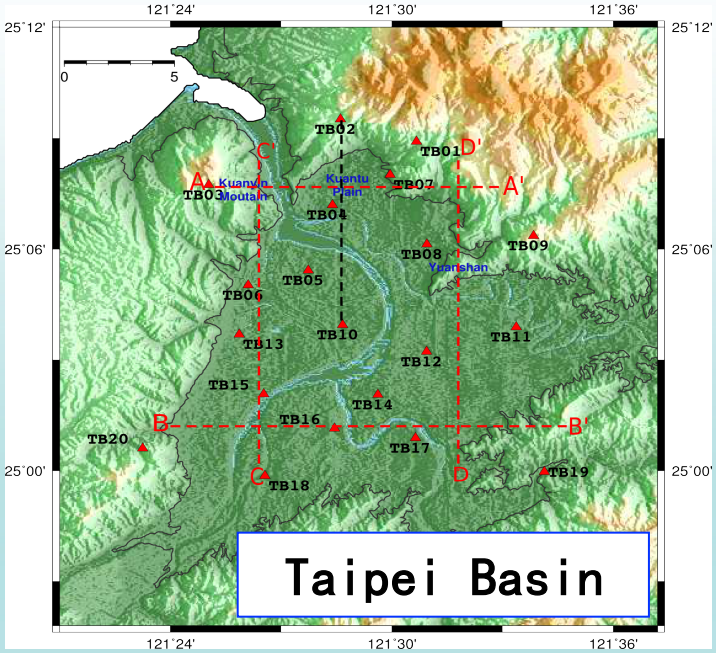

~ 10 x 10 km scale

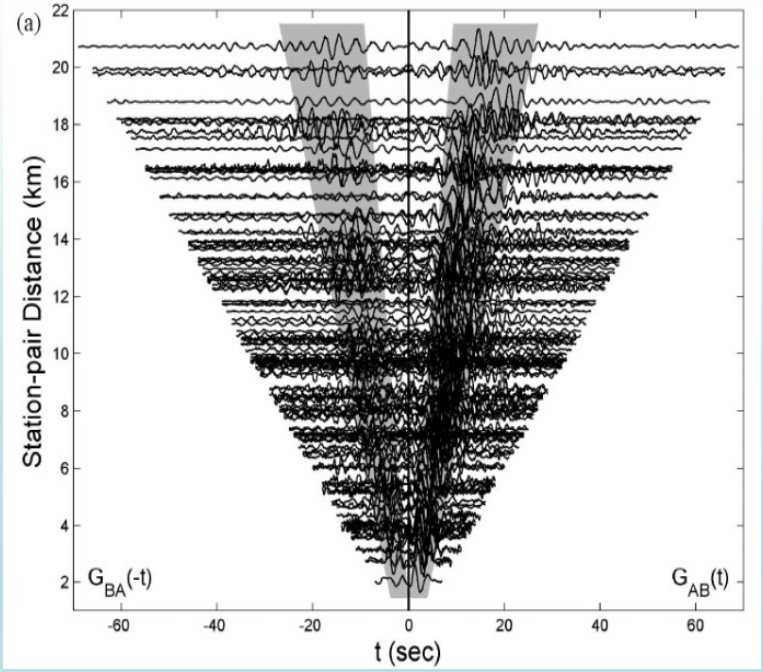

Period: 0.5-3 s

Ray path distribution using the final Vs model

T = 0.8 s

T = 1.4 s

T = 2.0 s

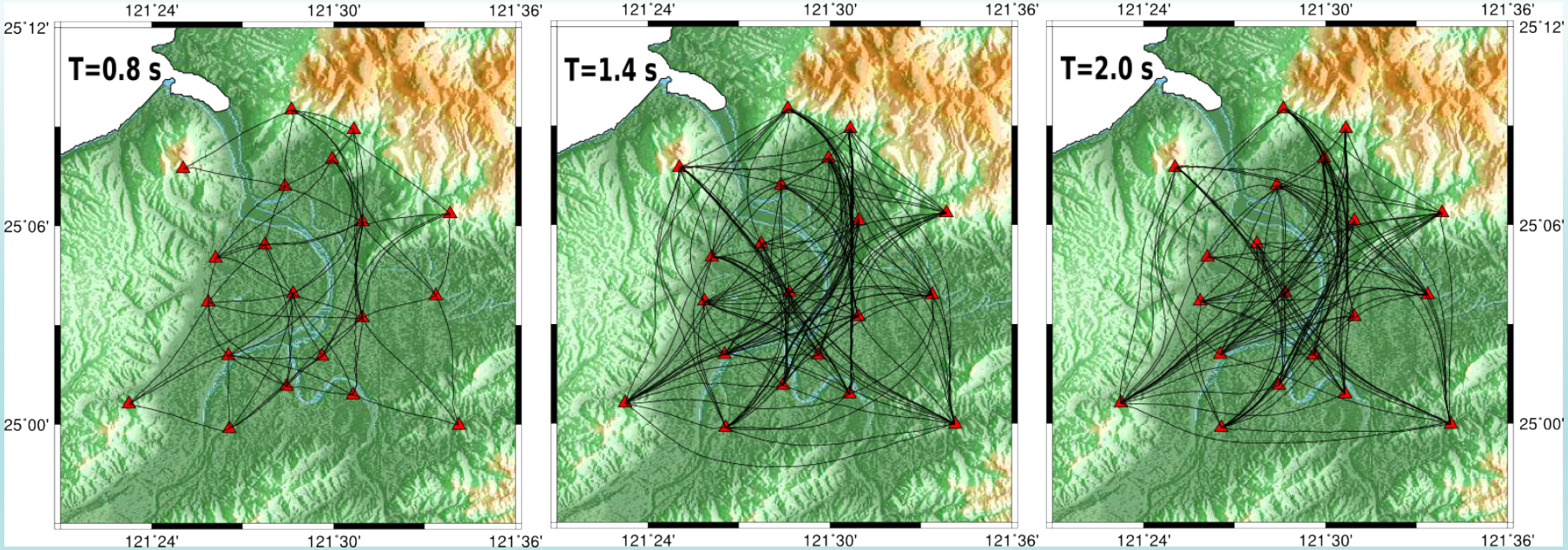

Strong effect of off-great-circle propagation!

3-D checkerboard resolution test

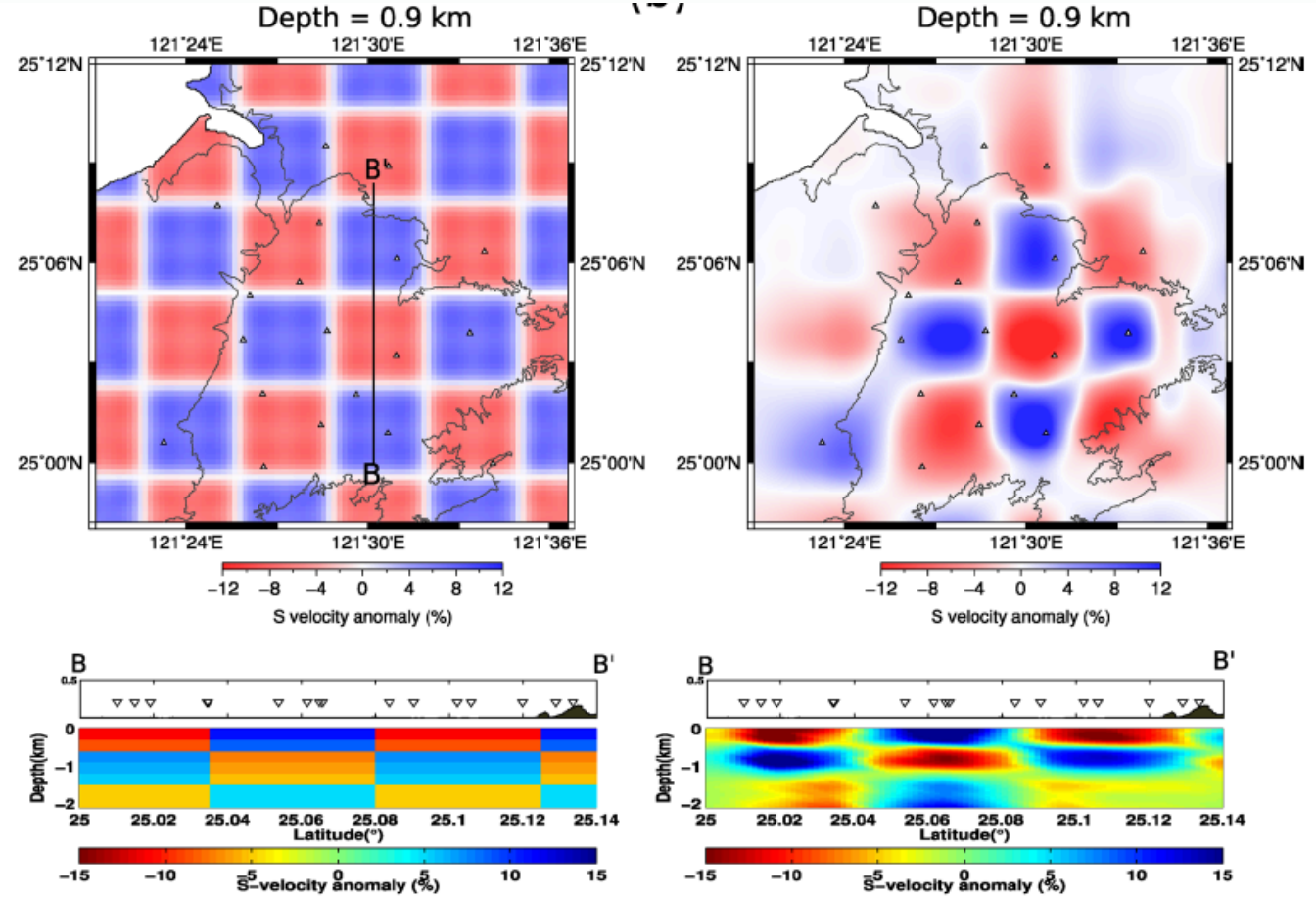

Inversion results along 4 profiles

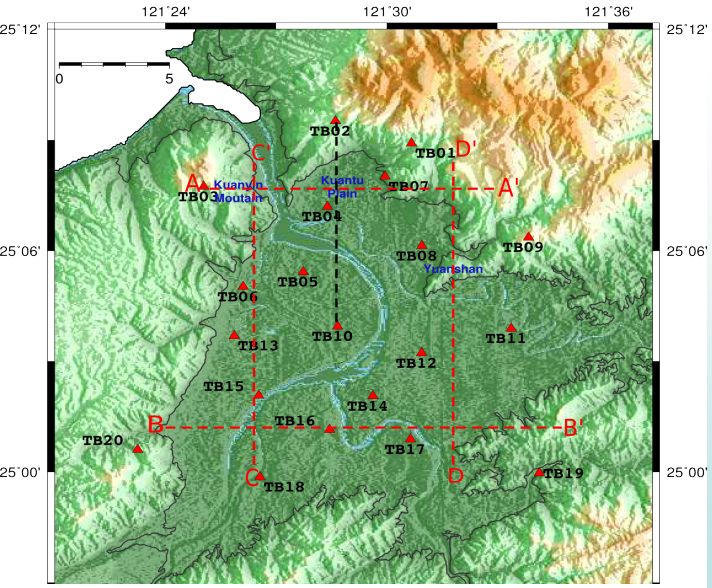

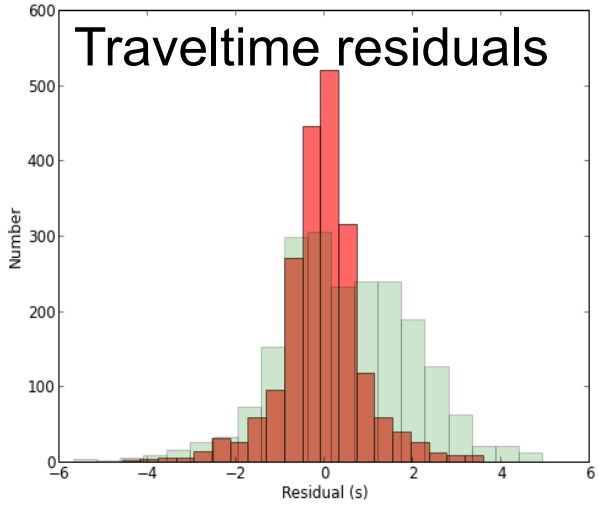

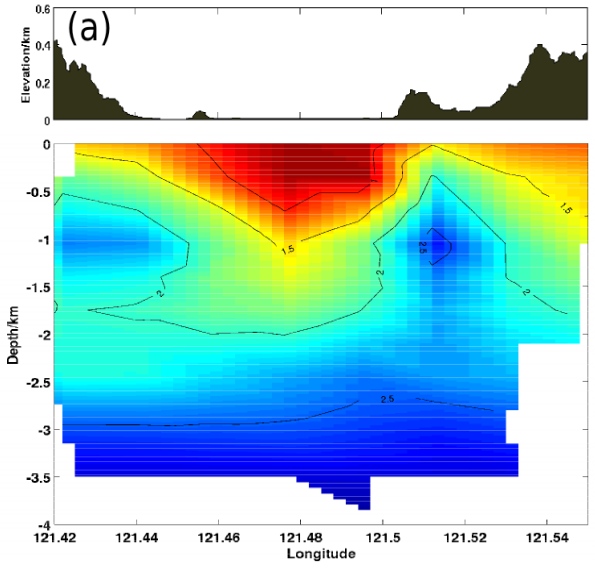

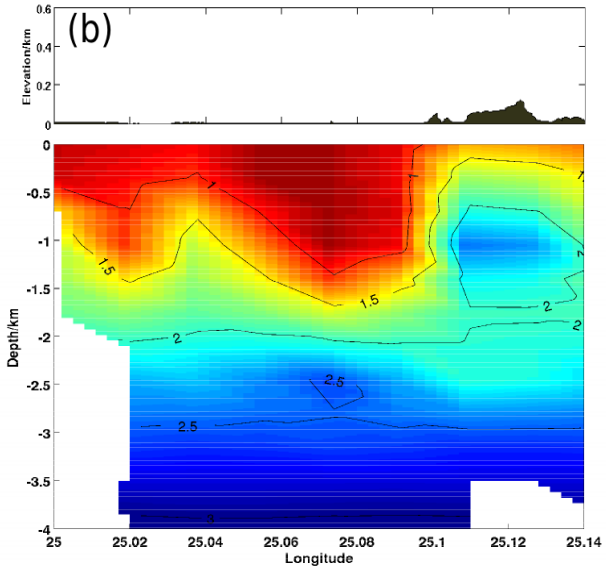

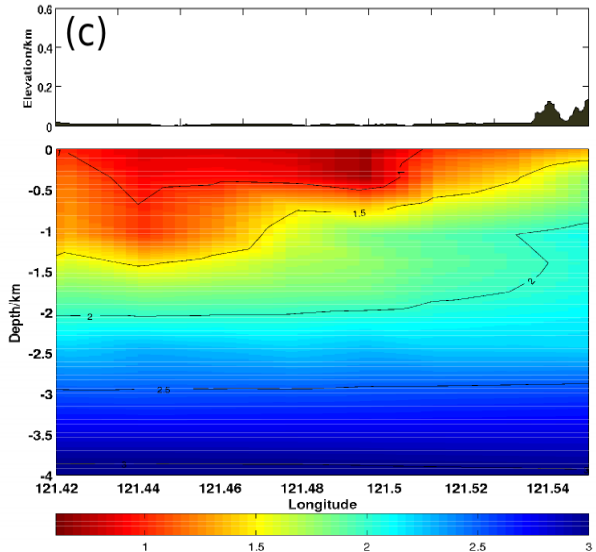

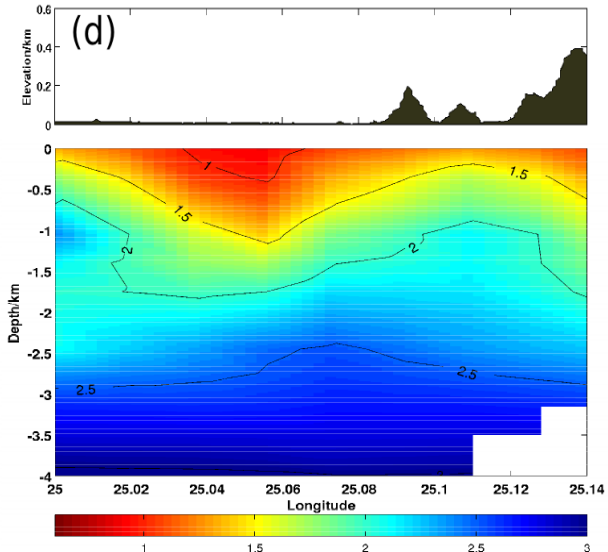

(2) Hefei urban area ambient noise tomography

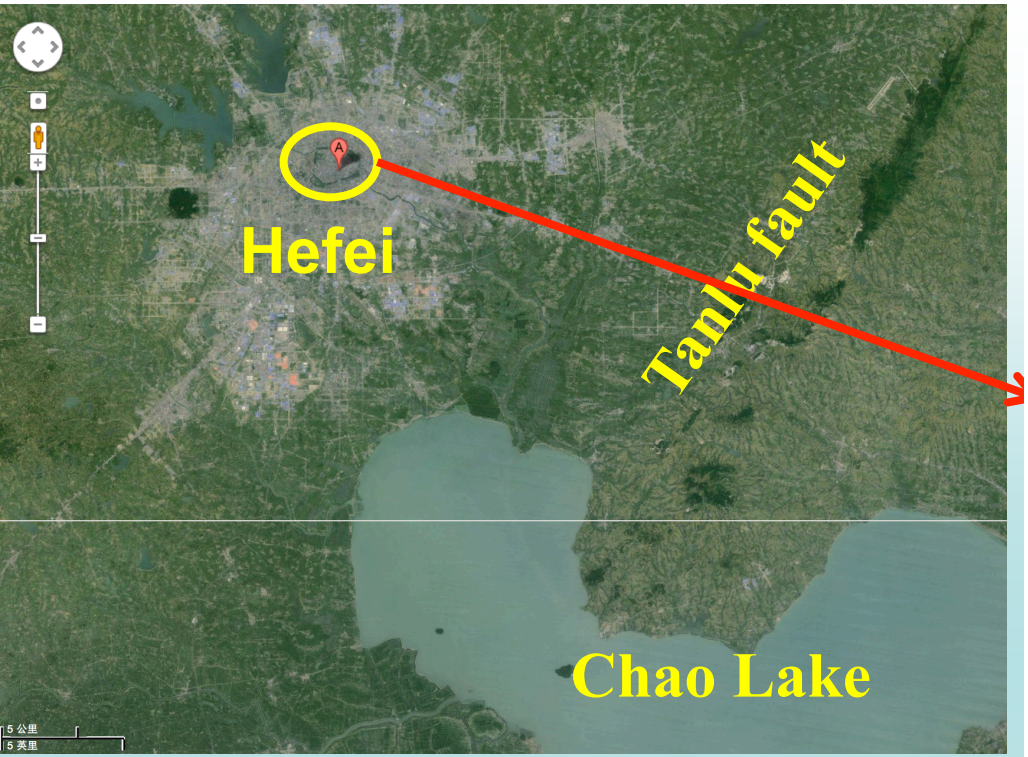

10 km

7 km x 5 km

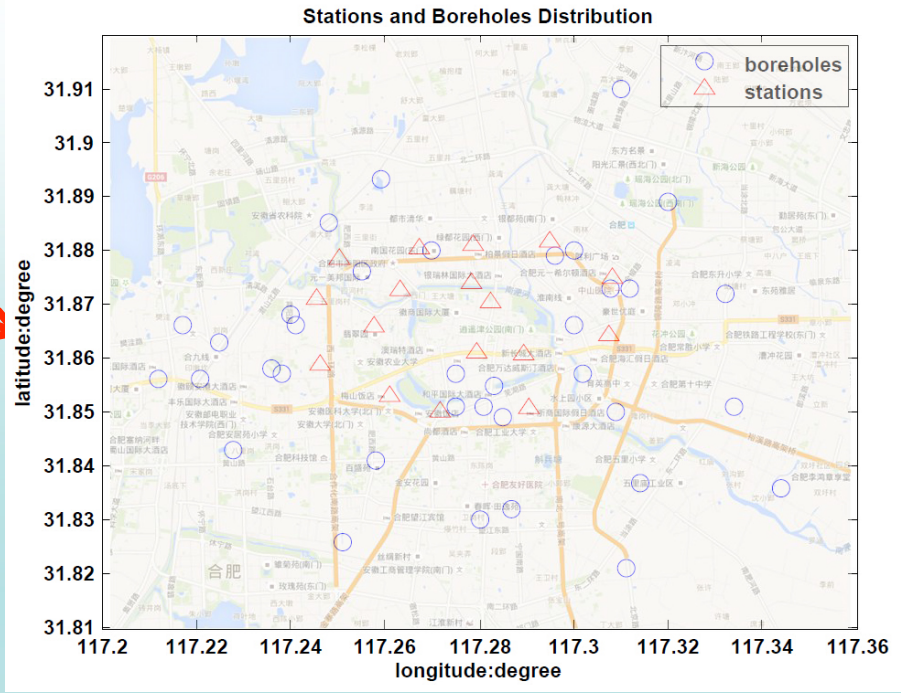

Station spacing about 0.5-2 km

17 stations, 2 weeks noise recordings

1-D shear wave velocity of boreholes

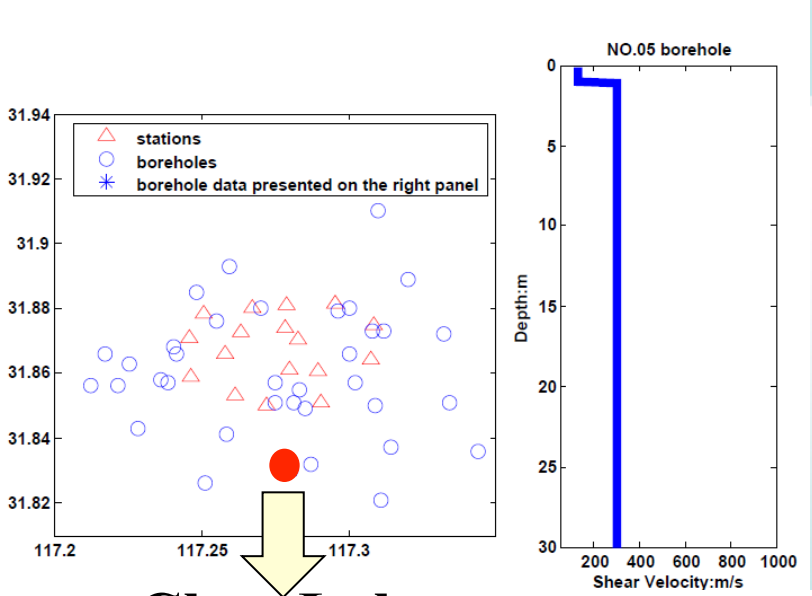

Chao Lake

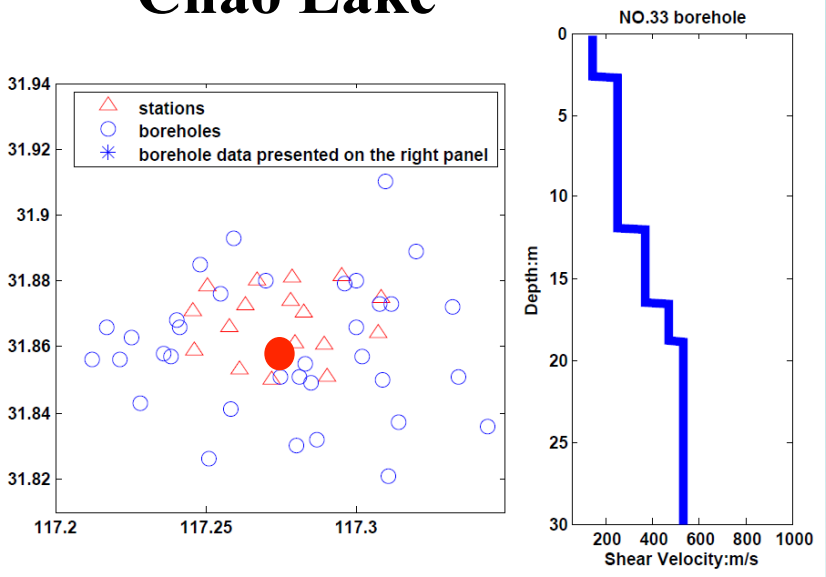

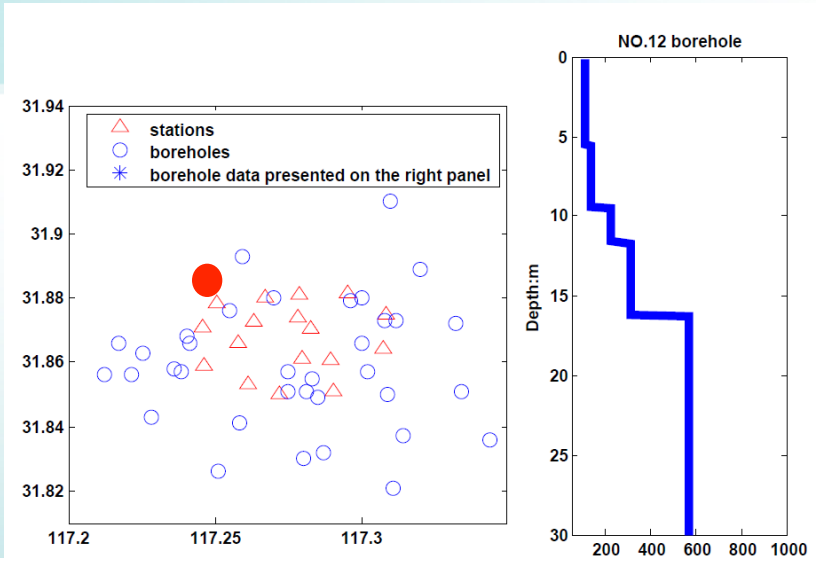

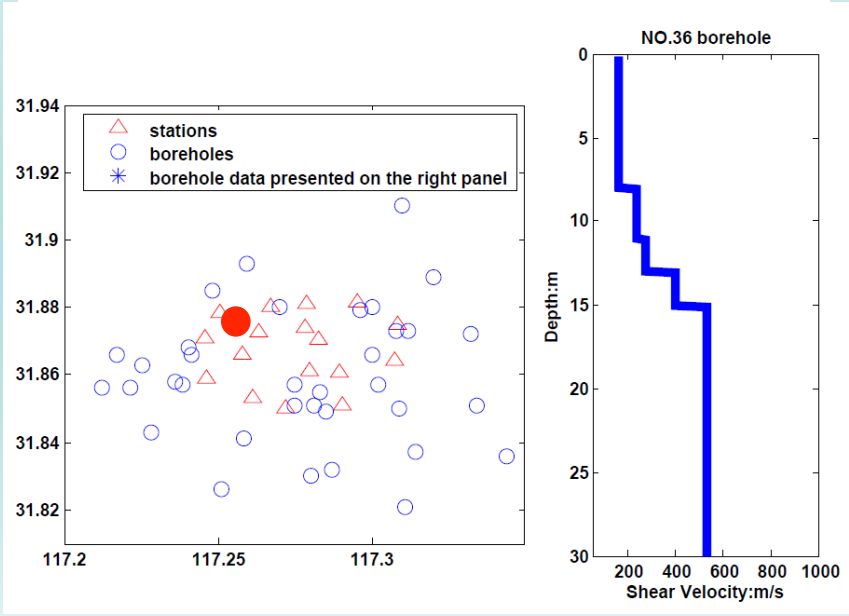

Ambient noise cross-correlation functions

Period band: 0.5 – 2 s
Stack hourly data Cross-Correlation Functions

normalized linear stacking method

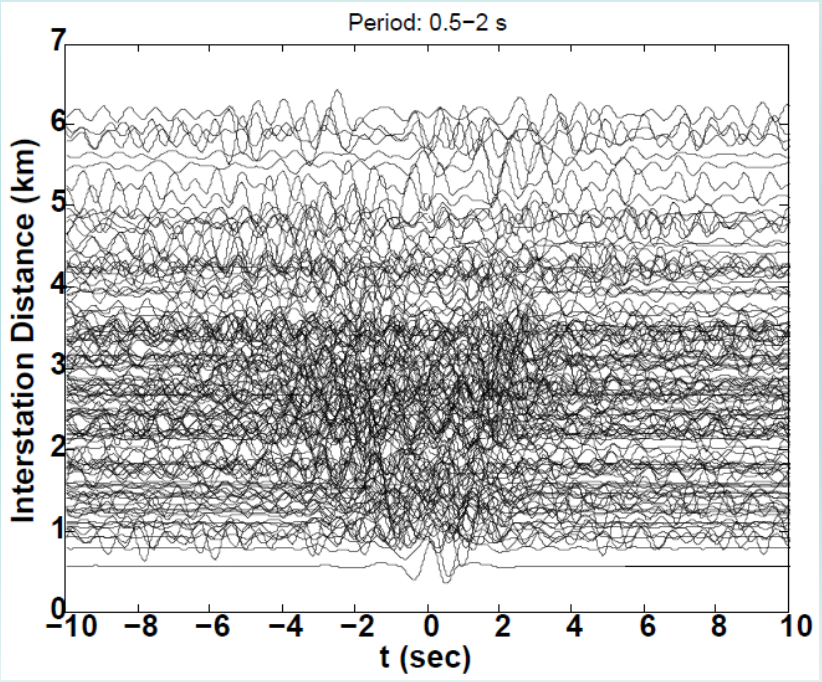

S-transform stacking method (Schimmel et al.,2011)

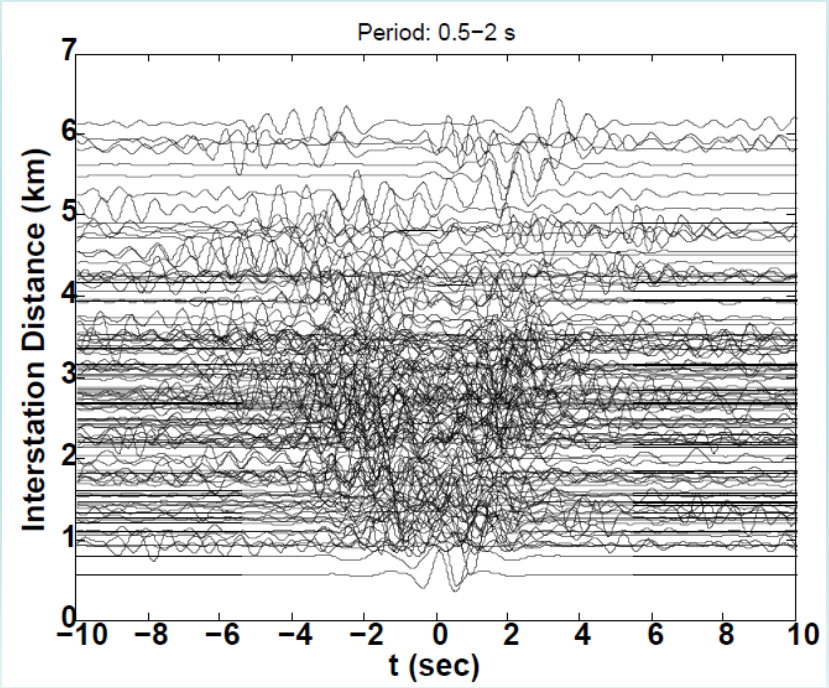

Joint phase + group travel time inversion results
(borehole data are incorporated in the initial model)

30m

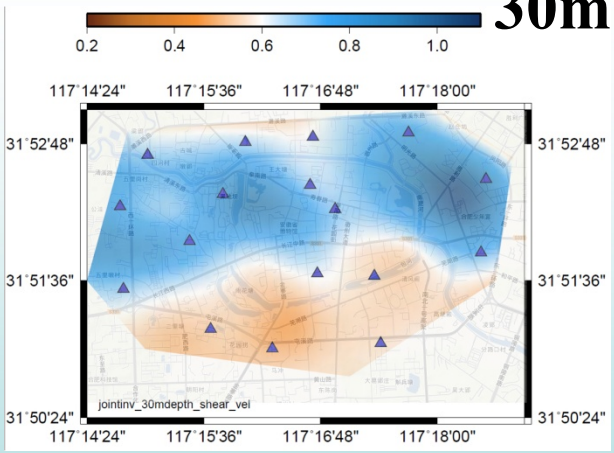

50m

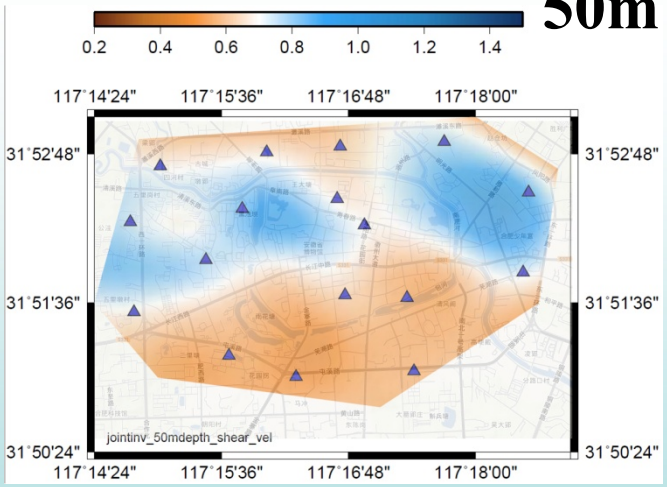

100m

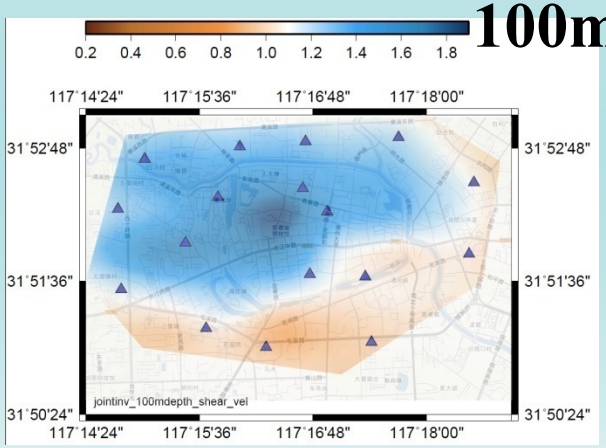

300m

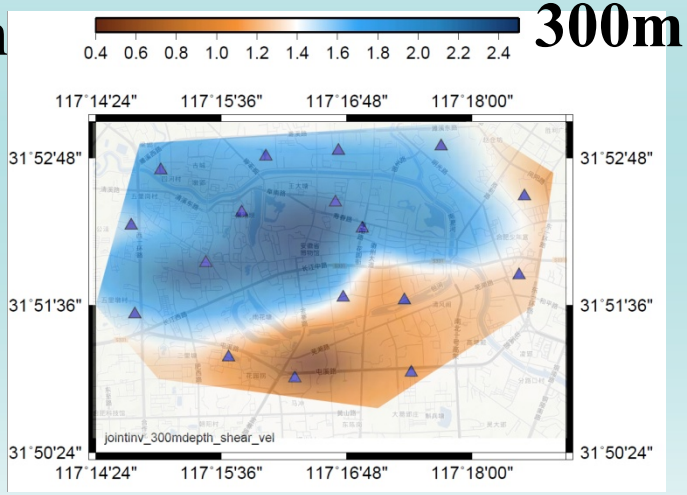

Ray path distribution

0.5 s

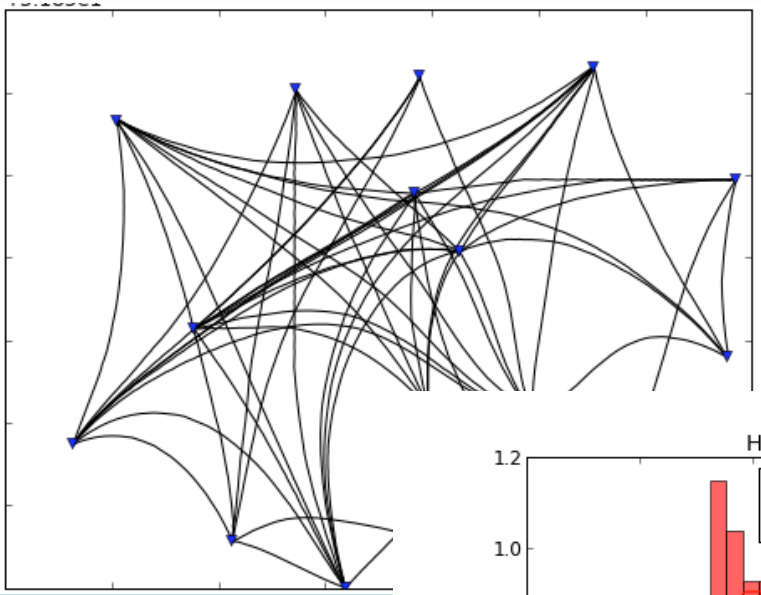

0.8 s

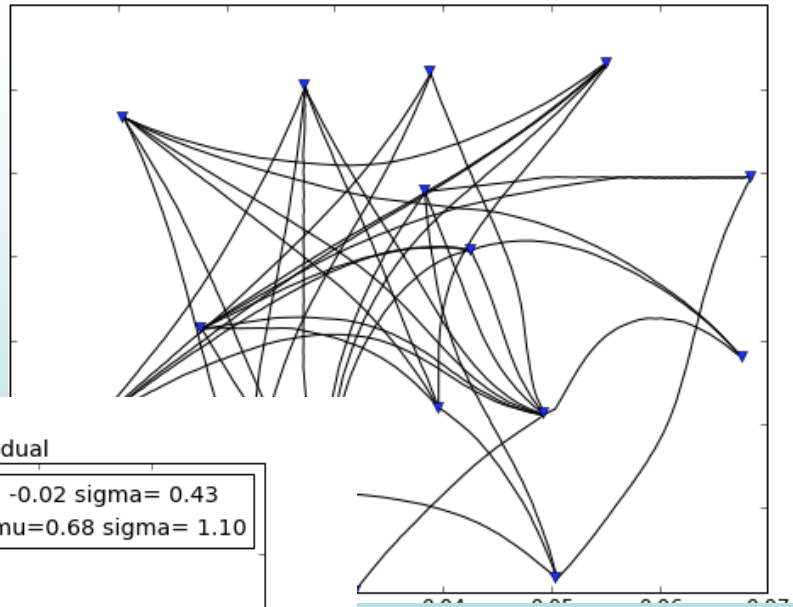

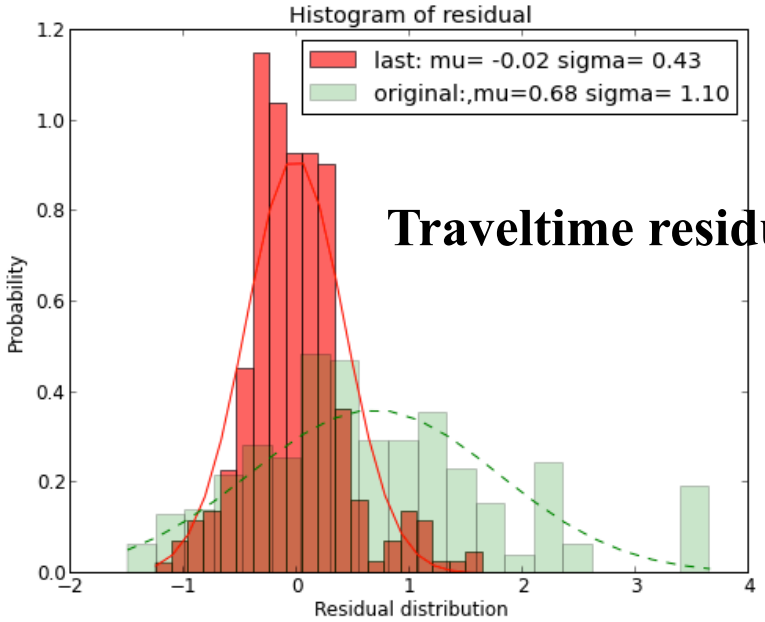

Traveltime residual

(3) Shale gas production field in SW China

45 stations

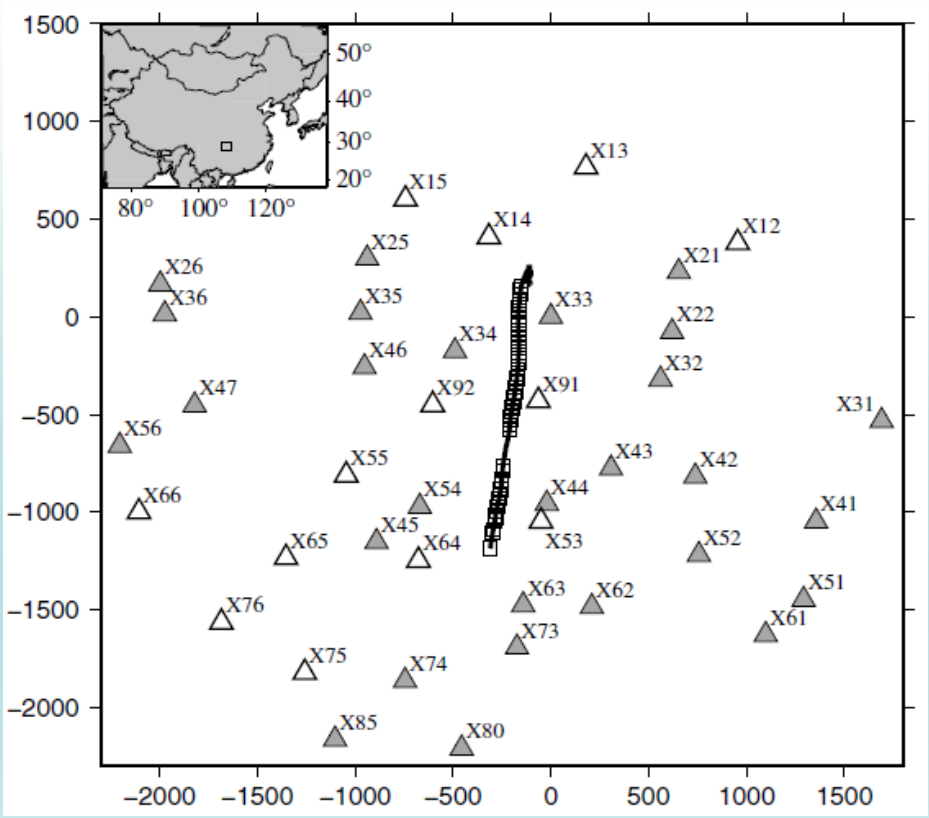

4 x 3 km

Cross-correlation from 10 days data

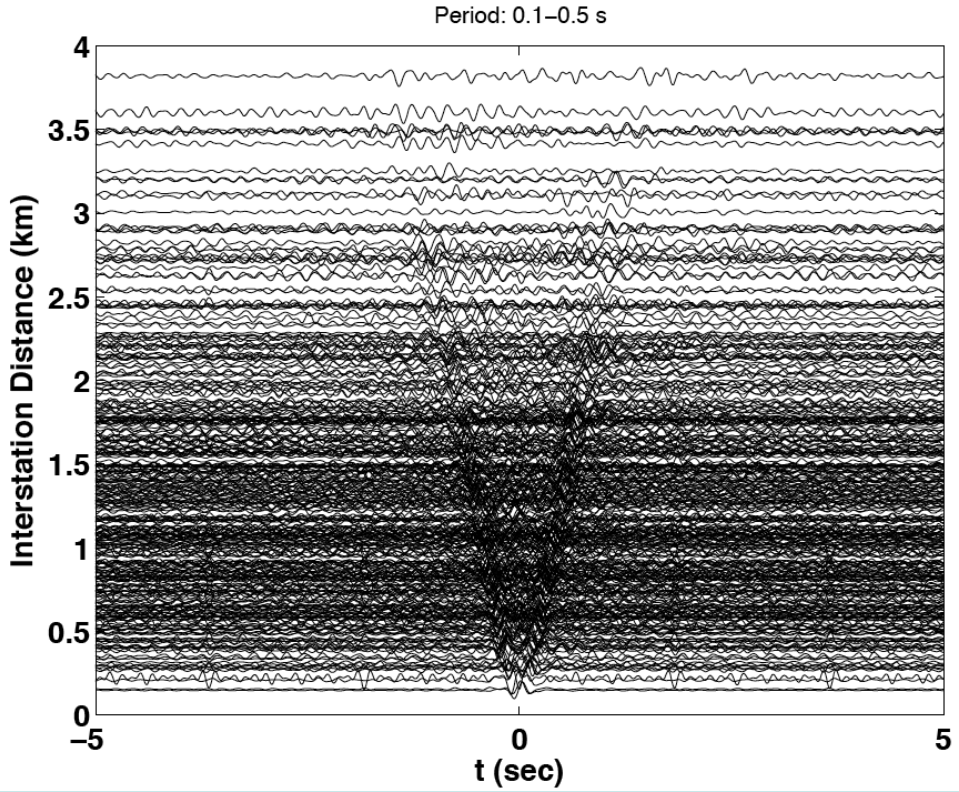

Period band: 0.1-0.5 s (2-10 Hz)
(sensitive to top half km structure)

Inversion results of Vs from dispersion data

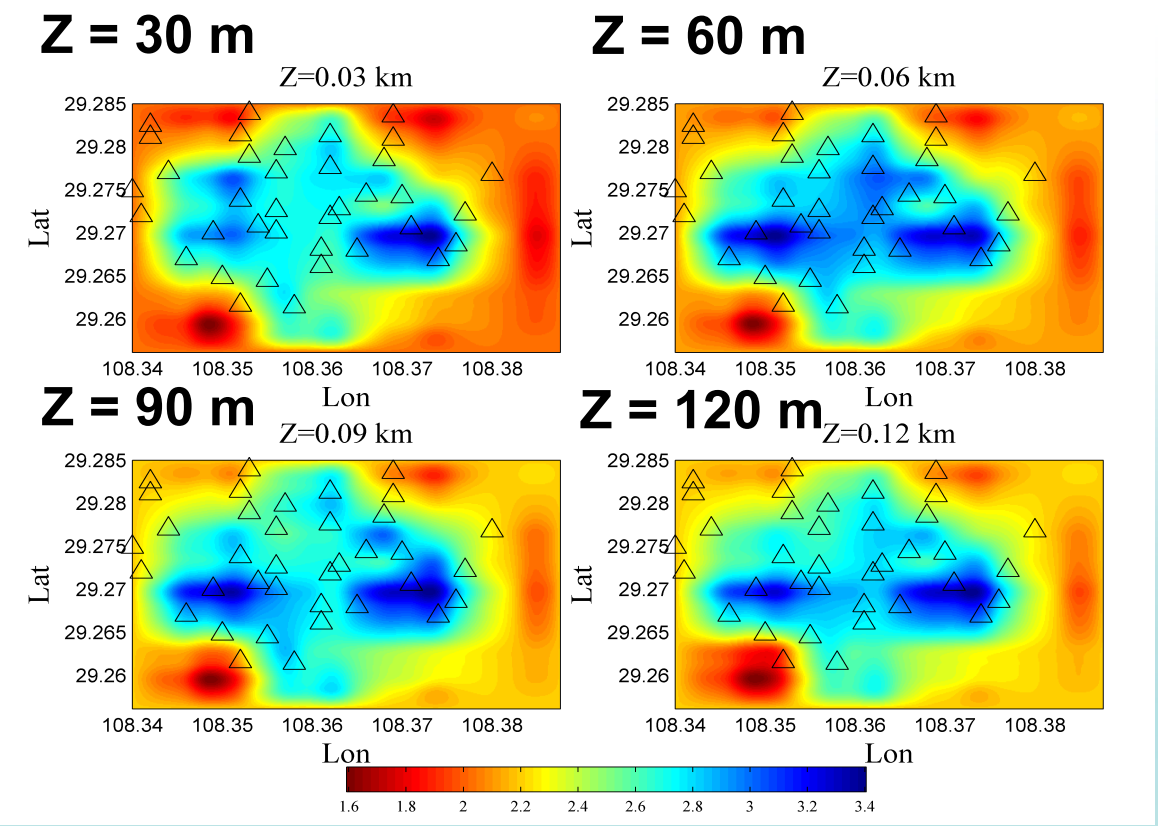

Provide important additional information (other than Vp) for characterizing oil/gas field structure

Provide a good starting model for full elastic waveform modeling and inversion

Topography effects on high-freq. surface wave tomography?

Topograhic Correction ? Full waveform inversion?

Outline

- Joint ambient noise and earthquake surface wave tomography (isotropic and anisotropic crust and upper mantle structures)

- Direct ambient noise/surface wave travel time tomography with ray tracing and wavelet-based inversion

- **Joint ambient noise and body wave travel time tomography**

Joint inversion of body wave arrival times and surface wave traveltime data (space domain)

$$\begin{bmatrix} \mathbf{G}_H^{T_p} & \mathbf{G}_{Vp}^{T_p} & \mathbf{0} \\ \mathbf{G}_H^{T_s} & \mathbf{0} & \mathbf{G}_{Vs}^{T_s} \\ \mathbf{0} & \mu\mathbf{G}_{V_p}^{SW} & \mu\mathbf{G}_{V_s}^{SW} \end{bmatrix} \begin{bmatrix} \mathbf{\Delta H} \\ \mathbf{\Delta m}_p \\ \mathbf{\Delta m}_s \end{bmatrix} = \begin{bmatrix} \mathbf{d}^{T_p} \\ \mathbf{d}^{Ts} \\ \mu\mathbf{d}^{SW} \end{bmatrix}.$$

$$\mathbf{Gm=d}$$

- Vp is solved by both first P-arrival times and surface wave data

- Vs is solved by both first S-arrival times and surface wave data

Joint inversion of body wave traveltime and surface wave traveltime data (wavelet domain)

$$\begin{bmatrix} \mathbf{G}_H^{T_p} & \mathbf{G}_{Vp}^{T_p} & \mathbf{0} \\ \mathbf{G}_H^{T_s} & \mathbf{0} & \mathbf{G}_{Vs}^{T_s} \\ \mathbf{0} & \mu\mathbf{G}_{V_p}^{SW} & \mu\mathbf{G}_{V_s}^{SW} \end{bmatrix} \begin{bmatrix} \mathbf{\Delta H} \\ \mathbf{\Delta m}_p \\ \mathbf{\Delta m}_s \end{bmatrix} = \begin{bmatrix} \mathbf{d}^{T_p} \\ \mathbf{d}^{Ts} \\ \mu\mathbf{d}^{SW} \end{bmatrix}.$$

$$\mathbf{Gm=d}$$

Wavelet domain

$$min.||\tilde{\mathbf{G}}\tilde{\mathbf{m}} - \mathbf{d}||_2^2 + \lambda||\tilde{\mathbf{m}}||_1$$

Solved by Iteratively Reweighted Least Square method

$$\mathbf{m} = \mathbf{W}^{-1}\tilde{\mathbf{m}}$$

Application to San Jacinto Fault Zone (SJFZ) (Preliminary)

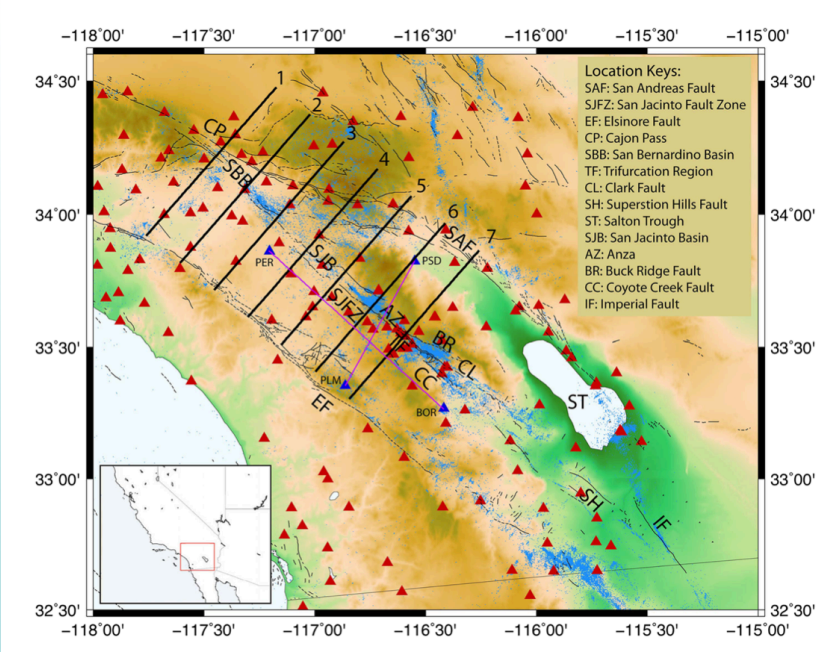

DD tomography (Allam and Ben-Zion, 2012; Allam et al., 2014)

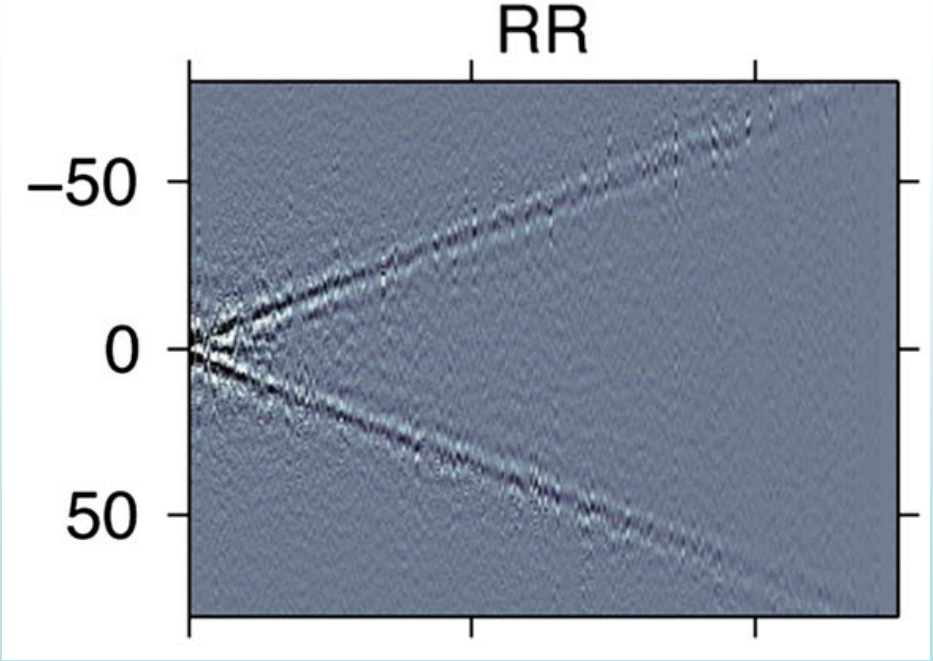

Ambient noise tomography (Rayleigh wave, 3-12s; Zigone et al., 2014)

Collaboration with the Ben-Zion's group at USC

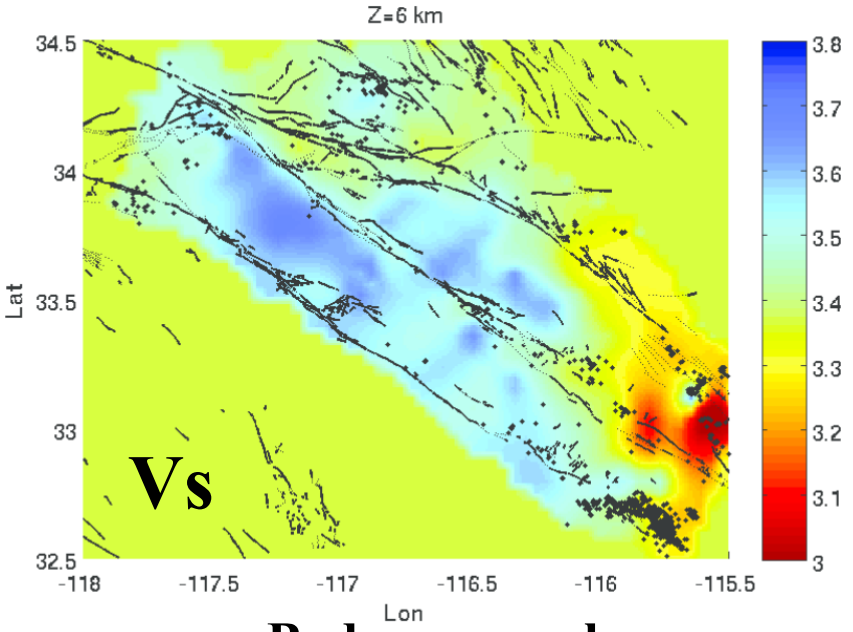

Body wave only

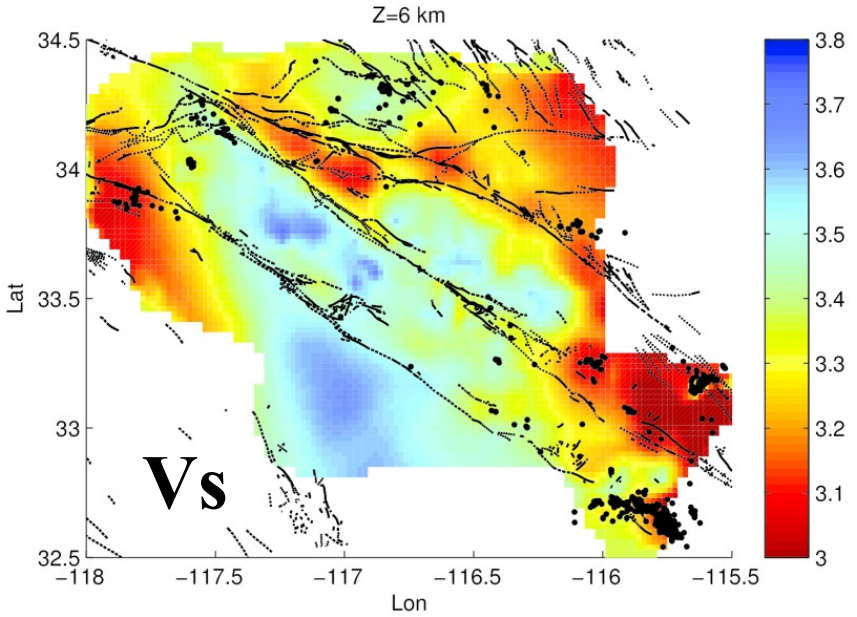

Joint inversion in space domain

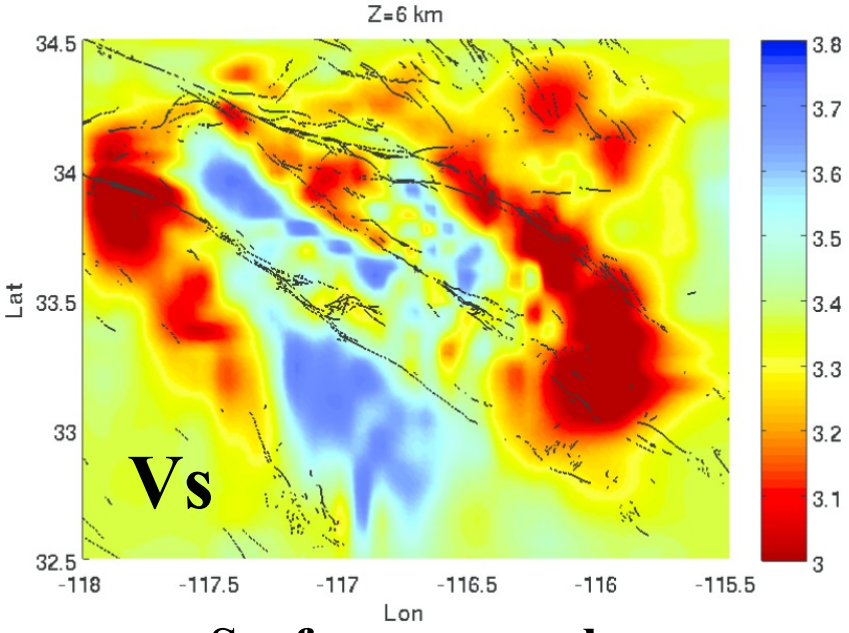

Surface wave only

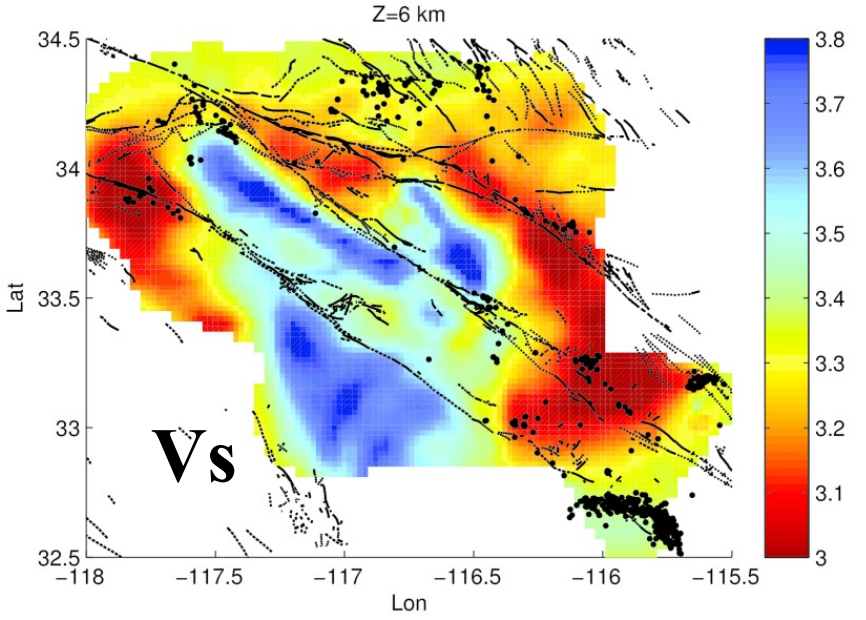

Joint inversion in wavelet domain

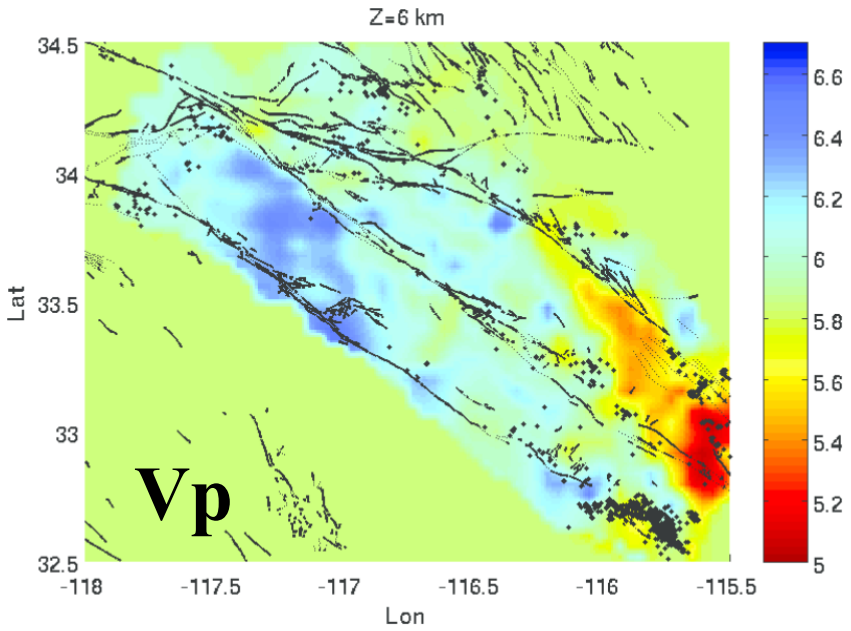

Body wave only

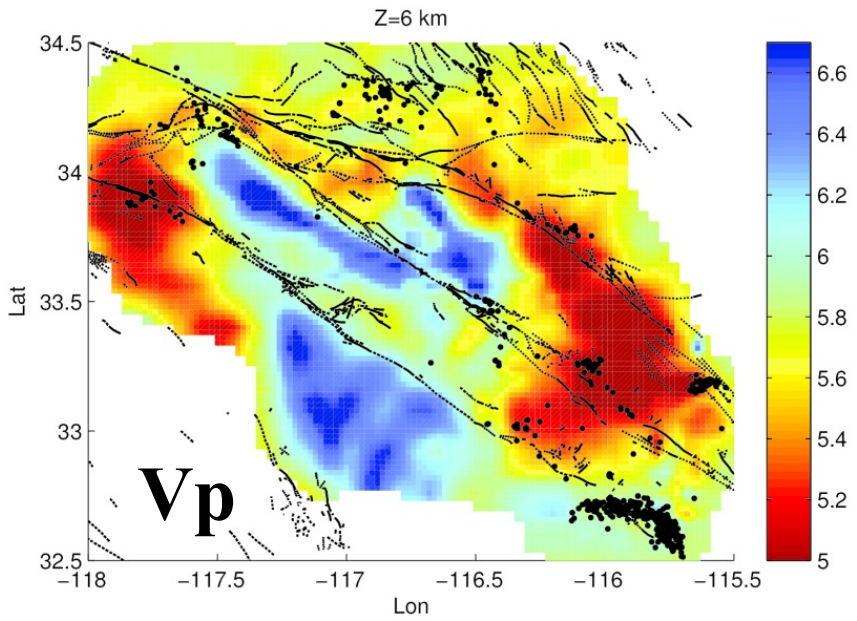

Joint inversion in wavelet domain

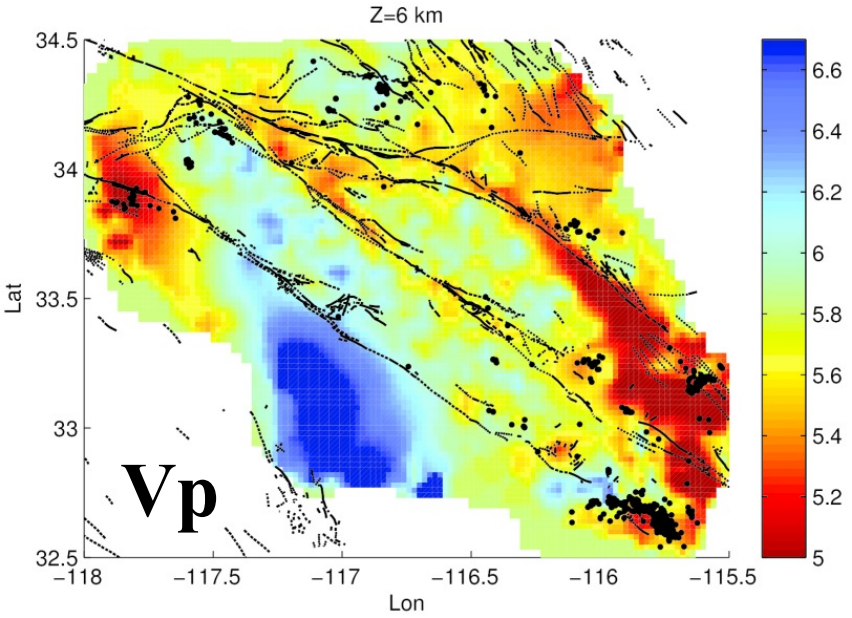

Joint inversion in space domain

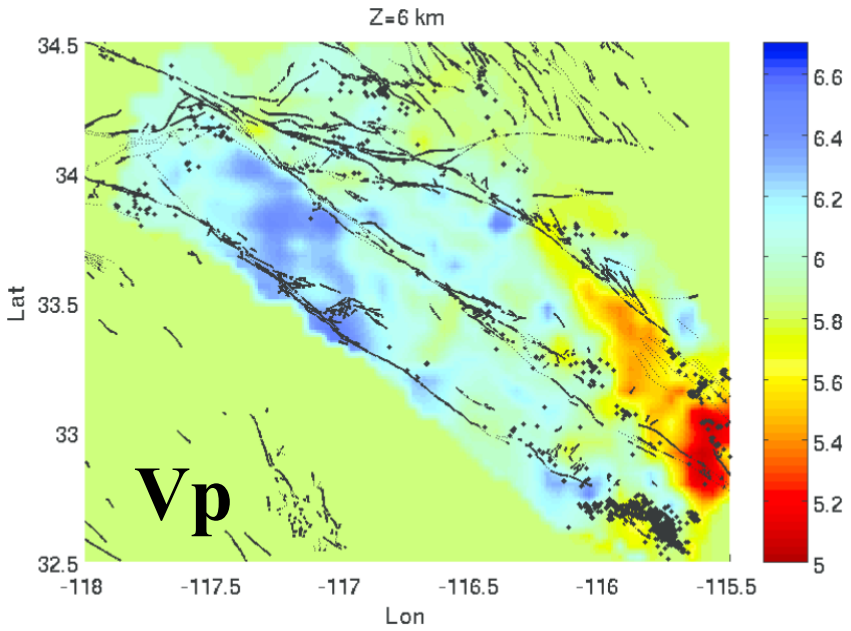

Body wave only

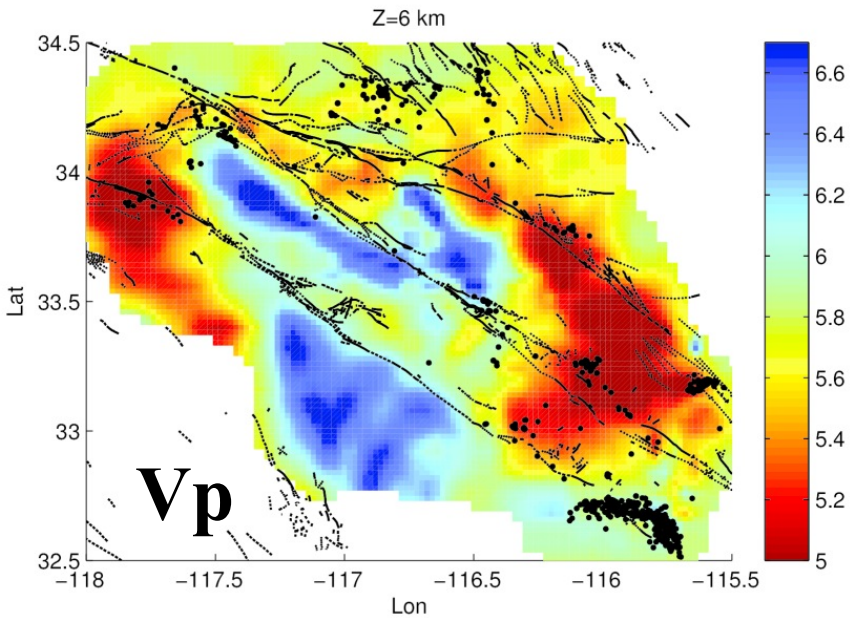

Joint inversion in wavelet domain

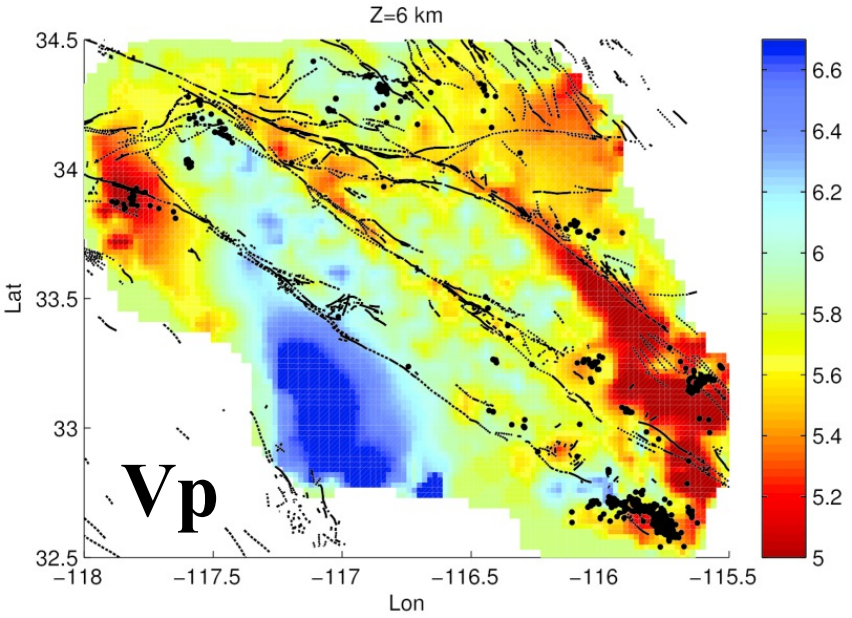

Joint inversion in space domain

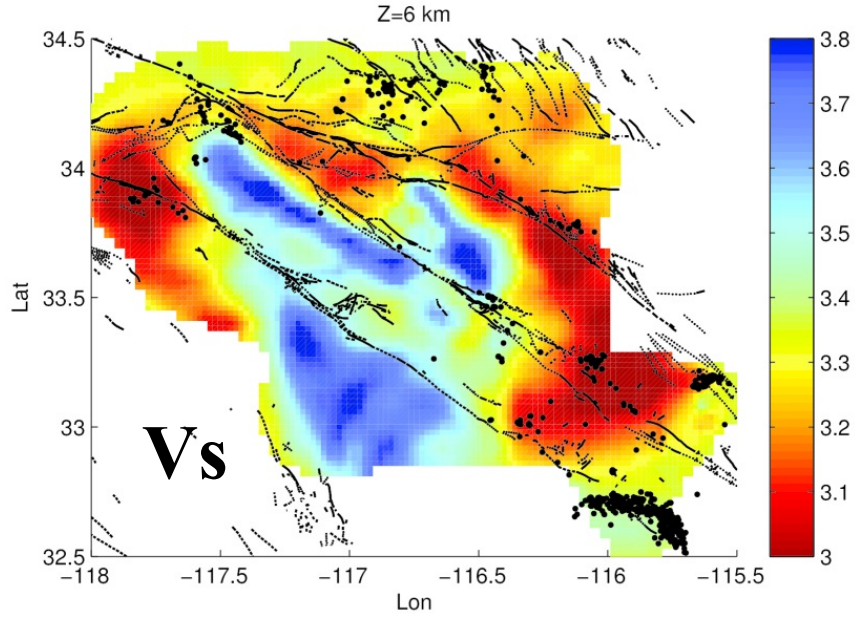

Joint inversion in wavelet domain

Joint inversion with more dataset

- ZH ratios (Rayleigh wave ellipticity): better constraints on shallow crustal structure and maybe density
- Receiver functions: better constraints on interfaces and average Vp/Vs ratios

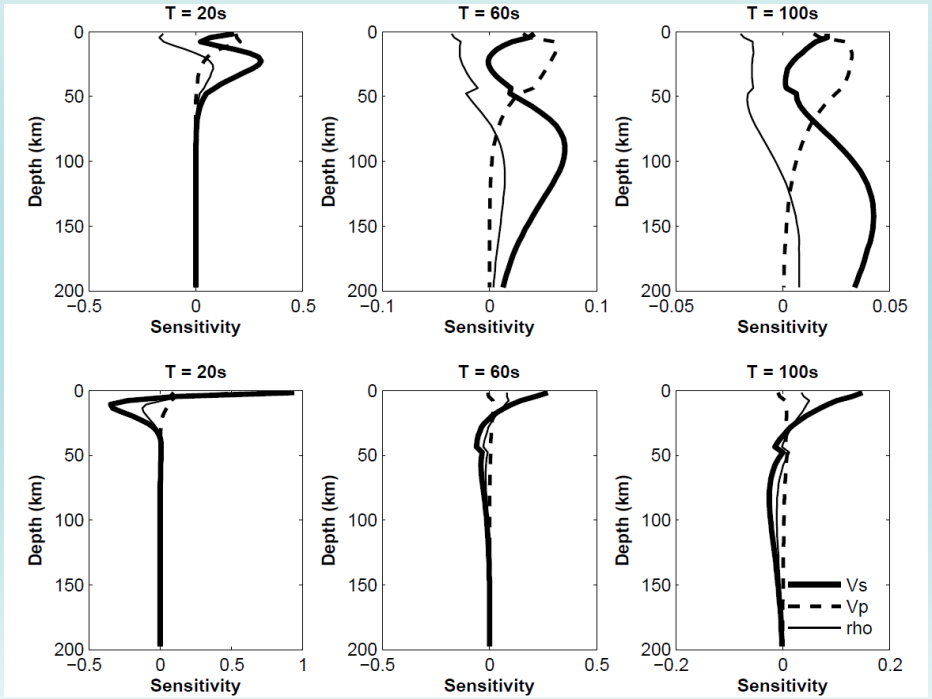

Phase v kernels

ZH ratio kernels

Joint inversion with more dataset

- ZH ratios (Rayleigh wave ellipticity): better constraints on shallow crustal structure and maybe density
- Receiver functions: better constraints on interfaces and average Vp/Vs ratios

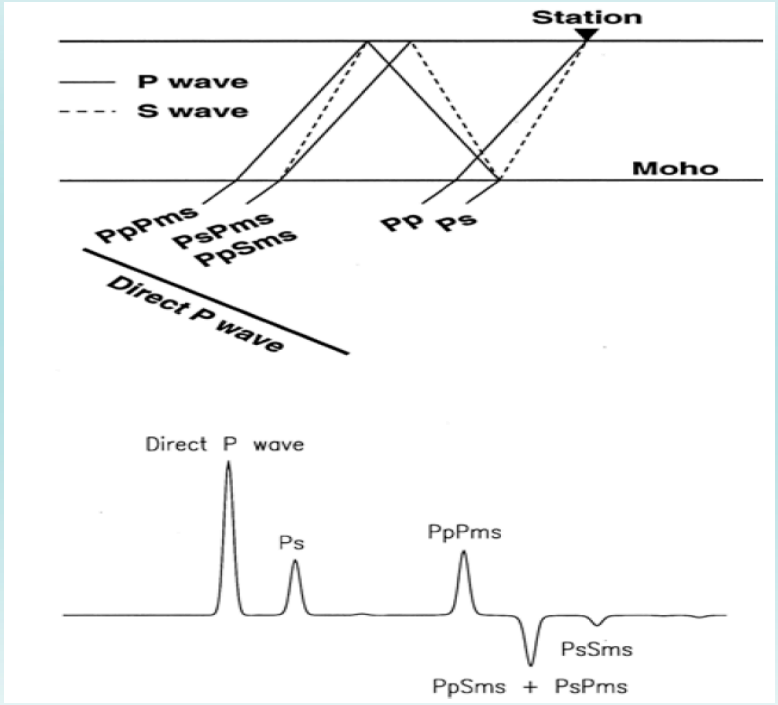

Conclusions

- Joint ambient noise and earthquake surface wave analyses provide better constraints on both crust and upper mantle structure and anisotropy.
- The proposed direct surface wave/ambient noise traveltime tomography for 3-D Vs structure takes accounts for ray bending effects of surface wave at different periods and can provide more accurate estimation of complex shallow crustal structure.
- The joint inversion of surface wave and body wave traveltimes enable us to explore more consistent Vp and Vs models.

Thank you!

hjyao@ustc.edu.cn
http://staff.ustc.edu.cn/~hjyao/

References

- Fang H., **Yao, H**.*, Zhang H, Huang, YC, van der Hilst R.D., 2015. Direct inversion of surface wave dispersion for three-dimensional shallow crustal structure based on ray tracing: methodology and application. ***Geophys.J. Int***. 201,1251—1263
- Chen M., Huang H, **Yao, H**., van der Hilst R.D., Niu F., 2014. Low wavespeed zones in the crust beneath the SE Tibet revealed by ambient noise adjoint tomography, ***Geophys. Res. Lett.***, 41(2), 334—340
- Gouedard, P., **Yao, H.**, van der Hilst, R. D., Ernst F., 2012. Surface wave eikonal tomography in heterogeneous media using exploration data. ***Geophys.J. Int.***, 191(2), 781-788, doi: 10.1111/j.1365-246X.2012.05652.x
- **Yao, H**., Gouedard, P., McGuire, J., Collins, J. and van der Hilst, R.D., **2011.** Structure of young East Pacific Rise lithosphere from ambient noise correlation analysis of fundamental- and higher-mode Scholte-Rayleigh waves, ***Comptes Rendues Geoscience de l'Académie des Sciences***, 343, 571–583, doi:10.1016/j.crte.2011.04.004
- **Yao H.**, van der Hilst, R.D., Montagner, J.-P., 2010. Heterogeneity and anisotropy of the lithosphere of SE Tibet from surface wave array analysis, ***J. Geophys. Res.***, 115, B12307, doi:10.1029/2009JB007142
- **Yao H.**, Campman, X., de Hoop, M.V., van der Hilst, R.D., 2009. Estimation of surface-wave Green's function from correlations of direct waves, coda waves, and ambient noise in SE Tibet, ***Phys. Earth Planet. Inter.,*** 177, 1–11, *doi:10.1016/j.pepi.2009.07.002*
- **Yao, H.** and Van der Hilst, R.D., 2009. Analysis of ambient noise energy distribution and phase velocity bias in ambient noise tomography, with application to SE Tibet, ***Geophys.J. Int.***, 179(2), 1113—1132, 10.1111/j.1365-246X.2009.04329.x
- **Yao, H.**, Beghein, C., and Van der Hilst, R.D., 2008. Surface-wave array tomography in SE Tibet from ambient seismic noise and two-station analysis: II - Crustal and upper mantle structure. ***Geophys.J. Int.,*** 173(1), 205-219, doi: 10.1111/j.1365-246X.2007.03696.x.
- **Yao, H.**, van der Hilst R.D., and de Hoop, M.V., 2006. Surface-wave array tomography in SE Tibet from ambient seismic noise and two-station analysis : I - Phase velocity maps. ***Geophys.J. Int.,*** Vol. 166(2), 732-744, doi: 10.1111/j.1365-246X.2006.03028.x**.**